NACA RM E50E29

NACA

RESEARCH MEMORANDUM

ALTITUDE PERFORMANCE CHARACTERISTICS OF TAIL-PIPE BURNER WITH VARIABLE-AREA EXHAUST NOZZLE

By Emmert T. Jansen and H. Carl Thorman

Lewis Flight Propulsion Laboratory
Cleveland, Ohio

NATIONAL ADVISORY COMMITTEE
FOR AERONAUTICS
WASHINGTON

August 11, 1950
Declassified September 1, 1959

NATIONAL ADVISORY COMMITTEE FOR AERONAUTICS

RESEARCH MEMORANDUM

ALTITUDE PERFORMANCE CHARACTERISTICS OF TAIL-PIPE BURNER WITH VARIABLE-AREA EXHAUST NOZZLE

By Emmert T. Jansen and H. Carl Thorman

SUMMARY

An investigation of turbojet-engine thrust augmentation has been conducted in the NACA Lewis altitude wind tunnel to determine the effect of altitude and flight Mach number on the performance of a tail-pipe burner equipped with a variable-area exhaust nozzle. With the variable-area exhaust nozzle, approximately constant turbine-outlet temperature could be maintained at rated engine speed during operation of the tail-pipe burner over a range of tail-pipe fuel-air ratios and flight conditions. The flight conditions investigated were: flight Mach numbers from 0.23 to 1.52 at an altitude of 45,000 feet, flight Mach numbers from 0.21 to 0.76 at an altitude of 25,000 feet, and an average flight Mach number of 0.22 at altitudes from 15,000 to 45,000 feet.

At a given flight Mach number, with constant exhaust-gas temperature and turbine-outlet temperature, increasing the altitude lowered the tail-pipe combustion efficiency and raised the total fuel-air ratio and the specific fuel consumption, while the augmented thrust ratio remained approximately constant. At a given altitude, with constant exhaust-gas temperature and turbine-outlet temperature, increasing the flight Mach number raised the combustion efficiency and the augmented thrust ratio and lowered the total fuel-air ratio and the specific fuel consumption.

INTRODUCTION

As part of an extensive research program on thrust augmentation of turbojet engines, an investigation has been conducted to determine the performance characteristics of a tail-pipe-burner installation including a variable-area exhaust nozzle over a wide range of simulated flight conditions in the NACA Lewis altitude wind tunnel.

Previous investigations of this research program (references 1 to 4) have indicated the effect of flame-holder and fuel-system design and the effect of altitude and flight Mach number on tail-pipe-burner performance with a fixed-area exhaust nozzle. From these investigations, the most efficient flame-holder and fuel-system configuration was selected and investigated in a tail-pipe burner with a variable-area exhaust nozzle.

Data are presented to show the effects of tail-pipe fuel-air ratio, altitude, and flight Mach number on tail-pipe-burner performance at rated engine speed and approximately constant turbine-outlet temperature. Operational characteristics of the tail-pipe burner and variable-area exhaust nozzle are also reported.

APPARATUS

Engine

The J47 turbojet engine used in this investigation has a sea-level static thrust rating of 5000 pounds at an engine speed of 7900 rpm and a turbine-outlet temperature of 1275° F (1735° R). At this rating, the air flow is approximately 94 pounds per second. The main components of the standard engine are a 12-stage axial-flow compressor, eight cylindrical direct-flow type combustors, a single-stage turbine, and a tail pipe. The maximum diameter of the engine is 37 inches. The over-all length of the engine, with the standard tail-pipe and exhaust nozzle, is 165 inches.

Tail-Pipe Burner Assembly

The standard tail pipe and exhaust nozzle were replaced by a tail-pipe burner assembly $108\frac{1}{2}$ inches long (fig. 1), which included a variable-area exhaust nozzle. The over-all length of the engine and tail-pipe-burner assembly was $218\frac{1}{2}$ inches. Details of the tail-pipe burner assembly with diffuser inner body and flame holder are shown in figure 2. The assembly consists of three sections: (1) a diffuser 41 inches long having an outlet-to-inlet area ratio of 1.9; (2) a combustion chamber $57\frac{1}{4}$ inches long composed of two cylindrical sections 24 and $25\frac{3}{4}$ inches long and 32 and 29 inches in diameter, respectively, connected by a transition section $7\frac{1}{2}$ inches in

length; and (3) a variable-area exhaust nozzle approximately $10\frac{1}{4}$ inches long in the full-open position. The projected outlet area of the nozzle was variable between 257 and 452 square inches. The combustion-chamber-inlet diameter of 32 inches, which was required for low-velocity flow at the flame holder, was not maintained over the entire length of the combustion chamber because the variable-area exhaust nozzle and the 29-inch-diameter rear section of the combustion chamber were supplied as a single unit by the engine manufacturer.

The diffuser and the combustion chamber were constructed of 0.063-inch Inconel. The downstream end of the diffuser inner body terminated at the combustion-chamber inlet in a blunt end 8 inches in diameter; a conical depression 4 inches deep at this point provided a sheltered region for seating a stabilizing flame in the center of the combustion chamber. A cooling liner constructed of 0.063-inch Inconel extended from the combustion-chamber inlet to within $1\frac{3}{8}$ inches of the outlet of the fixed portion of the exhaust nozzle. This cooling liner provided a 1/2-inch passage between the liner and the burner shell through which flowed 0.06 to 0.08 of the tail-pipe gas at approximately turbine-outlet temperature. The liner was supported in the cylindrical sections of the combustion chamber by methods that were designed to permit free longitudinal expansion of the liner (fig. 2(b)). Interlocking channels were used to support the cooling liner in the forward section of the combustion chamber. In order to permit rapid disassembly of the tail-pipe burner, the liner in the rear section was supported only by hat-section stiffeners. These stiffeners were seam-welded to the liner and were held against the burner shell at the combustion-chamber outlet by small clips extending $1\frac{1}{2}$ inches into each hat section.

The variable-area exhaust nozzle was constructed to give a single-plane circular outlet area when closed (fig. 3(a)) and also when full open (fig. 3(b)), except that in the open position the four corners of the movable lips protruded $1\frac{1}{2}$ inches into the circular area. At intermediate positions the outlet was irregular in shape. Thin metal sealing strips were provided between the fixed and movable portions of the nozzle to prevent leakage.

The fuel was injected normal to the direction of gas flow from 12 radial, streamlined tubes (fig. 4) equally spaced circumferentially around the diffuser section at a plane $26\frac{1}{2}$ inches

upstream of the flame holder. Each tube had 8 orifices 0.035 inch in diameter, thus providing an over-all pattern of 96 orifices equally distributed on four concentric circles. The outer circle of orifices was so located as to prevent fuel from entering the passage between the cooling liner and the burner shell.

A two-annular-V flame holder (fig. 5), which blocked 30 percent of the burner cross-sectional area, was installed at the forward end of the combustion chamber, as shown in figure 2. The inner diameter of the flame holder was considered the minimum that would prevent overheating of the flame holder by the stabilizing flame seated on the diffuser cone, and the outer diameter of the flame holder was considered the maximum that would prevent overheating the cooling liner.

The tail-pipe-burner ignition system used in this investigation was similar to "system B" in reference 1. This system incorporated an independently controlled fuel pump that provided instantaneous injection of fuel through the large-slot orifice of one of the engine fuel nozzles at a pressure of 100 to 200 pounds per square inch above the large-slot manifold pressure. The introduction of this excess fuel into the engine combustor produced a streak of flame through the turbine to ignite the fuel-air mixture in the tail-pipe burner.

INSTALLATION AND INSTRUMENTATION

The engine and tail-pipe burner assembly were mounted on a wing section that spanned the 20-foot-diameter test section of the altitude wind tunnel (fig. 1). Dry air was supplied from the tunnel make-up air system through a duct to the engine inlet. The inlet-air duct was connected to the engine by means of a frictionless slip joint, which permitted installation drag and thrust to be measured by the tunnel balance scales. In order to simplify the installation, no engine or tail-pipe-burner cowling was installed.

Instrumentation was installed at the engine inlet (station 1) and at the three stations (6, 7, and 8) in the tail-pipe-burner assembly shown in figure 2(a). Air flow was determined from the pressure and temperature measurements at the engine inlet, station 1. A complete pressure and temperature survey was obtained at the turbine outlet, station 6, and static-pressure measurements were made at the combustion-chamber inlet, station 7. Total and static pressures were measured at station 8, 1 inch upstream of

the outlet of the fixed portion of the exhaust nozzle, by means of a water-cooled survey rake. The drag of this rake was taken into account in the determination of scale jet thrust. Cross sections indicating the arrangement of instrumentation at stations 1, 6, and 8 are shown in figure 6. Instrumentation at station 7 consisted of four static-pressure wall orifices 90° apart on the circumference of the tail-pipe burner shell. Engine and tail-pipe fuel flows were measured by calibrated rotameters. The methods of calculation used to determine the engine and tail-pipe burner performance from these measurements are given in the appendix.

Fuel conforming to specification AN-F-32 (kerosene) with a lower heating value of 18,550 Btu per pound and a hydrogen-carbon ratio of 0.155, was used in the engine; fuel conforming to specification AN-F-48b, grade 80 (unleaded gasoline) with a lower heating value of 19,000 Btu per pound and a hydrogen-carbon ratio of 0.186, was used in the tail-pipe burner.

PROCEDURE

The tail-pipe burner was operated over a range of altitudes from 15,000 to 45,000 feet at an average flight Mach number of 0.22, over a range of flight Mach numbers from 0.21 to 0.76 at an altitude of 25,000 feet, and over a range of conditions that simulated flight Mach numbers from 0.23 to 1.52 at an altitude of 45,000 feet. The engine-inlet air temperature was regulated to correspond to the standard total temperature for each flight condition, except that the minimum average temperature obtained was about -5° F (455° R). The air flow through the inlet duct was throttled from approximately sea-level pressure to the total pressure at the engine inlet corresponding to the desired flight Mach number while the static pressure in the tunnel test section was maintained to simulate the desired altitude. A special technique was required for simulating flight conditions at an altitude of 45,000 feet for flight Mach numbers higher than 0.23 because of air-flow requirements of the engine and limitations of the tunnel-exhauster capacity. For these simulated-flight conditions, the pressure and the temperature at the engine inlet were regulated to correspond to the desired flight Mach number at an altitude of 45,000 feet but the ambient pressure in the tunnel test section was maintained at a value that corresponded to a lower altitude. The test-section ambient pressure was so selected, however, that the exhaust-nozzle outlet was always choked, with the result that the pressures in the engine were unaffected by test-section pressure. All the internal engine operating conditions therefore simulated those of

high-speed, high-altitude operation. The thrust obtained at the operating condition was adjusted to correspond to the thrust at 45,000 feet, as indicated in the appendix.

At each flight condition the engine was operated at rated speed while the tail-pipe fuel flow and the exhaust-nozzle-outlet area were simultaneously varied to maintain the turbine-outlet total temperature at approximately 1710° R. The temperature limit of 1710° R was selected instead of the rated temperature of 1735° R in order to provide a margin of safety during experimental operation.

RESULTS AND DISCUSSION

Results presented herein show the variation of combustion efficiency, exhaust-gas total temperature, augmented thrust ratio, and specific fuel consumption with tail-pipe fuel-air ratio at approximately constant turbine-outlet total temperature and at several different flight conditions. The augmented thrust ratio is defined as the net thrust with tail-pipe burning divided by the net thrust of the standard engine at identical engine operating conditions. The tail-pipe fuel-air ratio is defined as the ratio of tail-pipe fuel flow to the weight flow of unburned air entering the tail-pipe burner. Results are also cross-plotted for constant exhaust-gas total temperatures to show the variations of combustion efficiency, total fuel-air ratio, augmented thrust ratio, and specific fuel consumption with altitude and flight Mach number at constant turbine-outlet temperature. The performance data for all flight conditions are presented in table I.

For all data presented herein, the turbine-outlet temperature was within ±50° of 1710° R and examination of the data indicated no appreciable effect of this temperature variation on the tail-pipe-burner performance. Because the engine was operated at constant speed and at an approximately constant turbine-outlet total temperature, the velocity, gas flow, and total pressure at the turbine-outlet were approximately constant at each given flight condition.

Because of the limitations of the refrigeration equipment, the minimum engine-inlet temperature obtained in this investigation was approximately 455° R. This temperature is higher than the NACA standard total temperature for some of the low flight Mach number and high-altitude conditions (fig. 7). An analysis indicates that, for the range of conditions in which standard-

altitude temperature was not obtained, the tail-pipe burner performance obtainable with standard-altitude engine-inlet temperatures would have been superior to the performance reported herein. For a flight Mach number of 0.22 at altitudes of 35,000 and 45,000 feet, where the variation from standard temperature was greatest, operation at standard inlet temperatures for rated engine speed and constant turbine-outlet temperature would give an engine temperature ratio 15 percent higher and an adjusted engine speed 7 percent higher. Performance characteristics of the engine are such that the turbine-outlet pressure at these standard conditions would be approximately 10 percent higher than the turbine-outlet pressure obtained with an engine-inlet temperature of 455° R. The experimental results presented indicate that such an increase in turbine-outlet pressure would tend to raise the tail-pipe combustion efficiency and the exhaust-gas temperature for a given tail-pipe fuel-air ratio. The augmented thrust ratio for a given exhaust-gas temperature, however, would not be appreciably affected by the 15-percent change in engine-inlet absolute temperature because the augmented net thrust would increase approximately in proportion to the standard-engine net thrust. The specific fuel consumption, at a constant fuel-air ratio, would be reduced about 6 percent by the increase in augmented net thrust.

Effect of Altitude

The effect of altitude on the variation of performance with tail-pipe fuel-air ratio is shown in figure 8 for an average flight Mach number of 0.22. At a given tail-pipe fuel-air ratio, an increase in altitude resulted in a reduction of tail-pipe combustion efficiency, which decreased the exhaust-gas temperature and augmented thrust ratio and increased the specific fuel consumption. The decrease in tail-pipe combustion efficiency is primarily due to reductions in turbine-outlet total pressure, inasmuch as the turbine-outlet temperature and combustion-chamber-inlet velocity remained approximately constant for all flight conditions.

At each altitude, the exhaust-gas temperature, augmented thrust ratio, and specific fuel consumption increased with tail-pipe fuel-air ratio over the entire range investigated. The tail-pipe fuel-air ratio at which maximum combustion efficiency occurred increased from approximately 0.039 to 0.044 as the altitude was raised from 15,000 to 45,000 feet. For this increase in altitude the maximum efficiency was reduced from 0.81 to 0.58. When the tail-pipe fuel-air ratio was increased beyond the value at which peak combustion efficiency occurred, the increases in exhaust-gas temperature and augmented thrust ratio became less pronounced.

Data shown in the foregoing curves are cross-plotted in figure 9 to show the effect of altitude on performance at exhaust-gas temperatures of 2600°, 2800°, and 3000° R. The performance variation with altitude was similar for each exhaust-gas temperature. An increase in altitude was accompanied by a reduction in combustion efficiency and an increase in total fuel-air ratio. At an exhaust-gas temperature of 2800° R, the augmented thrust ratio, for a flight Mach number of 0.22, remained approximately constant at 1.26 but the specific fuel consumption increased from 2.25 to 2.96 as the altitude was increased from 15,000 to 45,000 feet. For the same change in altitude the standard-engine specific fuel consumption varied from 1.23 to 1.27.

Effect of Flight Mach Number

The effect of flight Mach number on the variation of performance with tail-pipe fuel-air ratio is shown in figure 10 for an altitude of 25,000 feet and in figure 11 for an altitude of 45,000 feet. At each altitude, the increases in turbine-outlet pressure that accompanied increases in flight Mach number raised the combustion efficiency for a given tail-pipe fuel-air ratio and thereby increased the exhaust-gas temperature. At a given fuel-air ratio the augmented thrust ratio also increased with flight Mach number at each altitude. At an altitude of 25,000 feet and fuel-air ratios above 0.045, the flight Mach number had no apparent effect on the specific fuel consumption. At an altitude of 45,000 feet, however, the specific fuel consumption was reduced when the flight Mach number was increased at a given tail-pipe fuel-air ratio.

At each flight Mach number, the exhaust-gas temperature, augmented thrust ratio, and specific fuel consumption increased with tail-pipe fuel-air ratio over the entire range investigated. At an altitude of 25,000 feet, the tail-pipe fuel-air ratio at which maximum combustion efficiency was obtained decreased from 0.043 at a flight Mach number of 0.21 to 0.036 at a flight Mach number of 0.76. For this increase in flight Mach number the maximum efficiency increased from 0.78 to 0.87. At an altitude of 45,000 feet, the maximum combustion efficiency occurred at a tail-pipe fuel-air ratio of approximately 0.048 for flight Mach numbers from 0.63 to 1.52. For this increase in flight Mach number, the maximum efficiency increased from 0.71 to 0.76.

Data obtained at altitudes of 25,000 and 45,000 feet are cross-plotted in figures 12 and 13, respectively, to show the effect of

flight Mach number on performance at several constant exhaust-gas temperatures. The variation of performance with flight Mach number was similar for each exhaust-gas temperature and altitude.

At a constant exhaust-gas temperature, the tail-pipe combustion efficiency increased with flight Mach number and therefore the total fuel-air ratio was reduced. The augmented thrust ratio increased and the specific fuel consumption decreased with increasing flight Mach number at a constant exhaust-gas temperature. The specific fuel consumption of the standard engine, however, increased to a maximum at a flight Mach number of about 0.70 and remained approximately constant at higher flight Mach numbers. The highest augmented thrust ratio obtained in this investigation was 1.74 at a flight Mach number of 1.52, an altitude of 45,000 feet, and an exhaust-gas temperature of 3200° R. Corresponding values of tail-pipe combustion efficiency and specific fuel consumption were 0.76 and 2.52, respectively.

The friction pressure drop from station 6 to station 8 in the tail-pipe burner when inoperative was 0.056 of the total pressure at the turbine outlet, as compared with 0.032 for the standard-engine tail pipe. Calculations indicate that the thrust loss caused by this increase in tail-pipe pressure loss ranges from 3 percent at low flight Mach numbers to 1 percent at high flight Mach numbers.

The data obtained in this investigation substantiate the results of previous investigations, such as reference 2, in that the tail-pipe combustion efficiency is adversely affected by reductions in turbine-outlet pressure and that the effect is most severe at pressures below about 1000 pounds per square foot. In order to illustrate this trend, data from figures 8, 10, and 11 have been cross-plotted in figure 14. At a constant tail-pipe fuel-air ratio of 0.040, decreasing the turbine-outlet total pressure from 2400 to 1000 pounds per square foot caused an average reduction in tail-pipe combustion efficiency of about 0.15, and when the pressure was reduced below 1000 pounds per square foot the combustion efficiency decreased at an accelerated rate. The maximum combustion efficiencies were similarly influenced by turbine-outlet total pressure, although the fuel-air ratio at which maximum combustion efficiency was obtained increased as the pressure decreased.

Operational Characteristics

Tail-pipe-burner ignition. - Ignition of the tail-pipe-burner fuel by means of a flame streak from one of the engine combustors

proved to be an extremely reliable method in this investigation, as well as in previous investigations. With this ignition system, tail-pipe-burner combustion was consistently started at rated engine speed and at all flight conditions, provided that a combustible mixture was present. Over 150 such starts were made during the investigation. Inspections of the turbine showed no damage due to the use of this ignition system.

Range of tail-pipe fuel-air ratios. - With turbine-outlet temperatures of 1660° to 1760° R, tail-pipe combustion blow-out was not encountered in the range of tail-pipe fuel-air ratios and flight conditions investigated. Limiting-turbine-outlet-temperature operation with the exhaust nozzle fully open was obtained at all flight conditions except two at which overheating of the tail-pipe shell occurred (subsequently discussed). As previously indicated, the exhaust-gas temperature obtained with the exhaust nozzle fully open varied from 3400° R at high flight Mach numbers to 2800° R at the lowest flight Mach number and highest altitude. The tail-pipe fuel-air ratios required for these temperatures ranged from 0.058 to 0.045 and the corresponding total fuel-air ratios were 0.061 to 0.051. The results indicate that at flight conditions where no excessive shell temperatures were encountered the use of an exhaust nozzle with a larger fully open outlet area would have permitted an increase in the maximum fuel-air ratio with an attendant increase in the maximum exhaust-gas temperature. The minimum tail-pipe fuel-air ratio at which performance data were obtained was about 0.025. Because the augmented thrust ratios at this fuel-air ratio ranged from 1.25 at high flight Mach numbers to 1.0 at low flight Mach numbers, operation at lower fuel-air ratios was not considered of interest.

Tail-pipe-burner shell cooling. - The gas flow through the passage between the cooling liner and the burner shell provided adequate shell cooling at all flight conditions, except at a tail-pipe fuel-air ratio of approximately 0.045 and at an altitude of 15,000 feet and a flight Mach number of 0.22 and at an altitude of 25,000 feet and flight Mach numbers above 0.59, which correspond to turbine-outlet total pressures higher than 2000 pounds per square foot. A continuous liner approximately $5\frac{1}{2}$ feet long (fig. 2) was used throughout the investigation, during which the total operation time with tail-pipe burning was 17 hours. The condition of the liner after the completion of the investigation is shown in figure 15. The progressive buckling of the liner was much more severe in the rear section of the combustion chamber than in the forward section because: (a) The exhaust-gas temperature was

higher in the rear section; (b) the pressure difference across the liner was greater because of the reduction in combustion-chamber diameter; and (c) the hat-section stiffeners provided less support against collapsing of the liner than the interlocking channels. The burning of holes in the liner shown in figure 15 occurred during the last 2 hours of tail-pipe-burner operation. This damage resulted from localized high temperatures on the liner caused by excessive buckling that distorted the flow of cooling gas.

Warping of the exhaust nozzle, which caused the movable lips to bind and some of the thin metal sealing strips to burn away, was encountered in an earlier investigation with a variable-area exhaust nozzle identical to the one used in this investigation. In order to prevent such warping, the exhaust nozzle used in this investigation was supported by a rectangular steel frame (figs. 1 and 15(a)). With the exhaust nozzle so strengthened, no failures were encountered during the 17 hours of tail-pipe-burner operation.

SUMMARY OF RESULTS

Results of an investigation to determine the effect of altitude and flight Mach number, at rated engine speed and approximately constant turbine-outlet temperature, on the performance of a 32-inch-diameter tail-pipe burner equipped with a variable-area exhaust nozzle were as follows:

1. At a given tail-pipe fuel-air ratio, increasing the altitude from 15,000 to 45,000 feet with an average flight Mach number of 0.22 caused a substantial reduction in combustion efficiency, which resulted in corresponding reductions in exhaust-gas temperature and augmented thrust ratio and increases in specific fuel consumption. At a constant exhaust-gas temperature, this increase in altitude reduced the combustion efficiency and raised the total fuel-air ratio and specific fuel consumption, while the augmented thrust ratio remained approximately constant.

2. At a given tail-pipe fuel-air ratio, increasing the flight Mach number at altitudes of 25,000 and 45,000 feet raised the combustion efficiency, exhaust-gas temperature, and augmented thrust ratio and lowered the specific fuel consumption, except that at an altitude of 25,000 feet; flight Mach number had no apparent effect on the specific fuel consumption above a tail-pipe fuel-air ratio of 0.045. For a constant exhaust-gas temperature, an increase in flight Mach number at a given altitude increased the combustion efficiency and the augmented thrust ratio and reduced the total fuel-air ratio and the specific fuel consumption.

3. The variations in tail-pipe combustion efficiency with altitude and flight Mach number at a given tail-pipe fuel-air ratio were primarily due to the changes in turbine-outlet pressure, the combustion efficiency increasing with turbine-outlet pressure. The highest tail-pipe combustion efficiency obtained in this investigation was 0.87 at a tail-pipe fuel-air ratio of 0.036, a flight Mach number of 0.76, and an altitude of 25,000 feet.

4. A maximum augmented thrust ratio of 1.74 was obtained at a flight Mach number of 1.52 and an altitude of 45,000 feet with an exhaust-gas temperature of 3200° R, a tail-pipe combustion efficiency of 0.76, and a specific fuel consumption of 2.52.

5. The thrust loss due to the friction pressure drop across the tail-pipe burner when inoperative ranged from 3 percent of the net thrust obtainable with the standard tail pipe at low flight Mach numbers to 1 percent at high flight Mach numbers.

6. No tail-pipe-burner combustion blow-out was encountered in the range of operating conditions investigated.

7. Tail-pipe-burner shell cooling was adequate to permit limiting-turbine-outlet temperature operation with tail-pipe burning over the full range of exhaust-nozzle areas at all flight conditions except those at which the turbine-outlet pressure was higher than 2000 pounds per square foot.

Lewis Flight Propulsion Laboratory,
National Advisory Committee for Aeronautics,
Cleveland, Ohio.

APPENDIX - CALCULATIONS

Symbols

A	cross-sectional area, sq ft
B	thrust-scale balance force, lb
C_j	jet-thrust coefficient, ratio of scale jet thrust to rake jet thrust
C_T	thermal-expansion ratio, ratio of hot-exhaust-nozzle area to cold-exhaust-nozzle area
D	external drag of installation, lb
D_r	drag of exhaust-nozzle survey rake, lb
F_j	jet thrust, lb
F_n	net thrust, lb
$F_{n,e}$	standard-engine net thrust, lb
f/a	fuel-air ratio
g	acceleration due to gravity, 32.2 ft/sec^2
H	total enthalpy, Btu/lb
h_c	lower heating value of fuel, Btu/lb
M	Mach number
N	engine speed, rpm
N_{adj}	adjusted engine speed, rpm (engine speed divided by square root of ratio of absolute engine-inlet total temperature to absolute engine-inlet total temperature at NACA standard-altitude condition)
P	total pressure, lb/sq ft absolute
P_8'	total pressure at exhaust-nozzle survey station in standard-engine tail pipe, lb/sq ft absolute

p	static pressure, lb/sq ft absolute
p_s	tunnel-test-section static pressure, lb/sq ft absolute
R	gas constant, 53.4 ft-lb/(lb)($^{\circ}$R)
T	total temperature, $^{\circ}$R
T_i	indicated temperature, $^{\circ}$R
t	static temperature, $^{\circ}$R
V	velocity, ft/sec
W_a	air flow, lb/sec
W_c	compressor-leakage air flow, lb/sec
W_f	fuel flow, lb/hr
W_f/F_n	specific fuel consumption based on total fuel flow and net thrust, lb/(hr)(lb thrust)
W_g	gas flow, lb/sec
γ	ratio of specific heats for gases
η_b	combustion efficiency

Subscripts:

a	air
e	engine
f	fuel
g	gas
j	station at which static pressure of jet equals free-stream static pressure
m	fuel manifold
r	exhaust-nozzle survey rake

s	scale, condition at which scale thrust was measured
t	tail-pipe burner
x	inlet duct at frictionless slip joint
0	free-stream conditions
1	engine inlet
3	engine-combustor inlet
6	turbine outlet or diffuser inlet
7	tail-pipe combustion-chamber inlet or diffuser outlet, $3\frac{1}{2}$ inches upstream of flame holder
8	exhaust nozzle, 1 inch upstream of exhaust-nozzle fixed-portion outlet

Methods of Calculation

Temperatures. - Static temperatures were determined from indicated temperatures with the following relation:

$$t = \frac{T_i}{1 + 0.85\left[\left(\frac{P}{p}\right)^{\frac{\gamma-1}{\gamma}} - 1\right]} \tag{1}$$

where 0.85 is the impact recovery factor for the type of thermocouple used.

Flight Mach number and airspeed. - Flight Mach number and equivalent airspeed were calculated from engine-inlet total pressure and temperature by assuming complete free-stream total-pressure recovery.

$$M_0 = \sqrt{\frac{2}{\gamma_1 - 1}\left[\left(\frac{P_1}{p_0}\right)^{\frac{\gamma_1-1}{\gamma_1}} - 1\right]} \tag{2}$$

$$V_0 = M_0\sqrt{\gamma_1 gRT_1\left(\frac{p_0}{p_1}\right)^{\frac{\gamma_1-1}{\gamma_1}}} \tag{3}$$

Air flow. - Air flow at the engine inlet was determined from pressure and temperature measurements obtained in the inlet annulus by the following equation:

$$W_{a,1} = p_1 A_1\sqrt{\frac{2\gamma_1 g}{(\gamma_1-1)Rt_1}\left[\left(\frac{P_1}{p_1}\right)^{\frac{\gamma_1-1}{\gamma_1}} - 1\right]} \tag{4}$$

Air flow at station 3 was obtained by taking into account the measured air leakage at the last stage of the compressor in the following manner:

$$W_{a,3} = W_{a,1} - W_c \tag{5}$$

Gas flow. - Gas flow through the engine was determined as follows:

$$W_{g,6} = W_{a,3} + \frac{W_{f,e}}{3600} \tag{6a}$$

Gas flow through the tail-pipe burner was determined as follows:

$$W_{g,7} = W_{g,8} = W_{a,3} + \frac{W_{f,e} + W_{f,t}}{3600} \tag{6b}$$

Fuel-air ratio. - The tail-pipe fuel-air ratio used herein is defined as the weight flow of fuel injected in the tail-pipe burner divided by the weight flow of unburned air entering the tail-pipe burner. Weight flow of unburned air was determined by assuming that the fuel injected in the engine combustor was completely burned. By combining air flow, engine fuel flow, and tail-pipe fuel flow, the following equation for tail-pipe fuel-air ratio is obtained:

$$(f/a)_t = \frac{W_{f,t}}{3600\ W_{a,3} - \frac{W_{f,e}}{0.068}} \tag{7}$$

where 0.068 is the stoichiometric fuel-air ratio for the engine fuel.

The total fuel-air ratio for the engine and tail-pipe burner is

$$f/a = \frac{W_{f,e} + W_{f,t}}{3600\ W_{a,3}} \tag{8}$$

Combustion-chamber-inlet velocity. - Velocity at the combustion-chamber inlet was calculated from the continuity equation using the static pressure measured at station 7, approximately $3\frac{1}{2}$ inches upstream of the flame holder and assuming isentropic expansion between stations 6 and 7.

$$V_7 = \frac{W_{g,7} R T_6}{p_7 A_7} \left(\frac{p_7}{P_6}\right)^{\frac{\gamma_6 - 1}{\gamma_6}} \tag{9}$$

Combustion efficiency. - Tail-pipe combustion efficiency was obtained by dividing the enthalpy rise through the tail-pipe burner by the product of the tail-pipe fuel flow and the lower heating value of the tail-pipe fuel.

$$\eta_b = \frac{3600\ W_{g,8} \Delta H_{g,t}}{W_{f,t} h_{c,t}}$$

$$= \frac{3600\ W_{a,3} H_a \Big]_{T_l}^{T_j} + W_{f,e} H_{f,e} \Big]_{T_m}^{T_j} + W_{f,t} H_{f,t} \Big]_{T_m}^{T_j} - W_{f,e} h_{c,e}}{W_{f,t} h_{c,t}} \tag{10}$$

The fuel temperature T_m was constant at 540° R. The engine fuel was assumed to be burned completely in the engine; this

assumption involves an error of less than 0.5 percent in the value of tail-pipe combustion efficiency. The enthalpy of the combustion products was determined from the hydrogen-carbon ratio of the fuels by the method explained in reference 5, in which dissociation is disregarded.

Augmented thrust. - The augmented net thrust was calculated by subtracting the free-stream momentum of the inlet air from the jet thrust of the installation.

$$F_n = F_j - \frac{W_{a,1}}{g} V_0 \tag{11}$$

For the flight conditions at which the tunnel test-section static pressure was maintained to simulate the desired altitude, the jet thrust of the installation was determined from the balance-scale measurements by the following equation:

$$F_j = F_{j,s} = B + D + D_r + \frac{W_{a,1} V_x}{g} + A_x(p_x - p_s) \tag{12}$$

The last two terms represent momentum and pressure forces on the installation at the slip joint in the inlet-air duct. The external drag of the installation was determined from experiments with a blind flange installed at the engine inlet to prevent air flow through the engine.

For the conditions simulating high flight Mach numbers at an altitude of 45,000 feet, a method of adjusting the scale jet-thrust measurements from the tunnel-pressure altitude to an altitude of 45,000 feet was derived as follows: The ratio between the jet thrust at an altitude of 45,000 feet and the scale jet thrust at the tunnel-pressure altitude may be expressed in terms of gas flow, exhaust-gas temperature, and pressure by the equation

$$\frac{F_j}{F_{j,s}} = \frac{\frac{W_{g,8}}{g} C_j \sqrt{gR \frac{2\gamma_8}{\gamma_8 - 1} T_j \left[1 - \left(\frac{p_0}{p_8}\right)^{\frac{\gamma_8 - 1}{\gamma_8}}\right]}}{\frac{W_{g,8}}{g} C_{j,s} \sqrt{gR \frac{2\gamma_8}{\gamma_8 - 1} T_j \left[1 - \left(\frac{p_s}{p_8}\right)^{\frac{\gamma_8 - 1}{\gamma_8}}\right]}}$$

where the subscript s is used to denote conditions at the tunnel-pressure altitude at which the scale jet thrust was measured. Because the engine-inlet conditions are fixed and the exhaust nozzle is choked, the exhaust-gas temperature and the gas flow are constant. The relation between the jet thrust at an altitude of 45,000 feet and the scale jet thrust at the tunnel-pressure altitude therefore becomes

$$F_j = F_{j,s} \frac{C_j}{C_{j,s}} \sqrt{\frac{1 - \left(\frac{p_0}{P_8}\right)^{\frac{\gamma_8 - 1}{\gamma_8}}}{1 - \left(\frac{p_s}{P_8}\right)^{\frac{\gamma_8 - 1}{\gamma_8}}}} \tag{13}$$

A value of 308 pounds per square foot, corresponding to NACA standard pressure for an altitude of 45,000 feet, was used for the static pressure p_0. In using equation (13) the assumption was made that $C_j/C_{j,s} = 1$, because the jet-thrust coefficients were unavailable in the range of tail-pipe pressure ratios corresponding to the high flight Mach numbers at 45,000 feet. Because this assumption does not take into account the possible reduction in jet-thrust coefficient with increases in pressure ratio, the net thrusts presented for the high flight Mach numbers at 45,000 feet may be slightly higher than those actually obtainable and the specific fuel consumptions correspondingly lower. The effect on the augmented thrust ratio is negligible, however, because a similar assumption was applied to the calculation of standard-engine thrust.

Standard-engine thrust. - The standard-engine net thrust was calculated by subtracting the free-stream momentum of the inlet air from the jet thrust of the standard engine.

$$F_{n,e} = F_{j,e} - \frac{W_{a,1}}{g} V_0 \tag{14}$$

The jet thrust obtainable with the standard engine at rated engine speed was calculated from measurements of turbine-outlet total pressure and temperature and gas flow obtained during the tail-pipe burning program.

$$F_{j,e} = \frac{W_{g,6}}{g} C_j \sqrt{\frac{2\gamma_6}{\gamma_6 - 1} gRT_6 \left[1 - \left(\frac{p_0}{P_8'} \right)^{\frac{\gamma_6 - 1}{\gamma_6}} \right]} \qquad (15)$$

Experimental data from previous operation of the engine indicated that the total-pressure loss across the standard-engine tail pipe between stations 6 and 8 was approximately 0.032 P_6 at rated engine speed; therefore, $P_8' = 0.968\ P_6$. The coefficient C_j was obtained from the curve shown in figure 16(a), which was determined from calibration of the engine with a standard tail pipe and a fixed-area conical exhaust nozzle. For the conditions simulating high flight Mach numbers at an altitude of 45,000 feet, a value of 308 pounds per square foot was used for p_0, but the jet-thrust coefficient C_j was assumed equal to the jet-thrust coefficient corresponding to the pressure ratio at the tunnel-pressure altitude.

Exhaust-gas total temperature. - The total temperature of the exhaust gas was determined from scale jet thrust, exhaust-nozzle total pressure, and gas flow as follows:

$$T_j = \frac{gF_{j,s}^2}{C_j^2 W_{g,8}^2 \left(\frac{2R\gamma_8}{\gamma_8 - 1} \right) \left[1 - \left(\frac{p_s}{P_8} \right)^{\frac{\gamma_8 - 1}{\gamma_8}} \right]} \qquad (16)$$

The coefficient C_j for the variable-area exhaust nozzle was obtained from the curve shown in figure 16(b). The ratio of specific heats γ_8 was based on an estimated value of temperature obtained by using the scale jet thrust and the projected outlet area of the exhaust nozzle to determine the approximate momentum at the vena contracta.

Jet-thrust coefficient. - The jet-thrust coefficient C_j, as used in the foregoing equations, is a calibration factor that may be defined as the ratio of scale (actual) jet thrust to the jet thrust calculated from pressure measurements by assuming complete isentropic expansion of the exhaust jet.

$$C_j = \frac{F_{j,s}}{F_{j,r}} = \frac{F_{j,s}}{C_T A_8 M_8 M_j \gamma_8 p_8 \left(\frac{p_s}{p_8}\right)^{\frac{\gamma_8 - 1}{2\gamma_8}}} \qquad (17)$$

The value of M_8 is determined by P_8 and p_8; the jet Mach number M_j is determined by P_8 and p_s. The thermal-expansion ratio C_T was based on exhaust-nozzle skin temperature and obtained from reference 6. For the data presented herein the exhaust-nozzle skin temperature ranged from 1500° to 1900° R and the corresponding values of C_T varied from 1.016 to 1.026.

REFERENCES

1. Conrad, E. William, and Prince, William R.: Altitude Performance and Operational Characteristics of 29-Inch-Diameter Tail-Pipe Burner with Several Fuel Systems and Flame Holders on J35 Turbojet Engine. NACA RM E9G08, 1949.

2. Thorman, H. Carl, and Campbell, Carl E.: Altitude-Wind-Tunnel Investigation of Tail-Pipe Burner with Converging Conical Burner Section on J35-A-5 Turbojet Engine. NACA RM E9I16, 1950.

3. Golladay, Richard L., and Bloomer, Harry E.: Altitude Performance and Operational Characteristics of 29-Inch-Diameter Tail-Pipe Burner with Several Fuel Systems and Fuel-Cooled Stage-Type Flame Holders on J35 Turbojet Engine. NACA RM E50A19, 1950.

4. Fleming, William A., and Wallner, Lewis E.: Altitude-Wind-Tunnel Investigation of Tail-Pipe Burning with a Westinghouse X24C-4B Axial-Flow Turbojet Engine. NACA RM E8J25e, 1948.

5. Turner, L. Richard, and Lord, Albert M.: Thermodynamic Charts for the Computation of Combustion and Mixture Temperatures at Constant Pressure. NACA TN 1086, 1946.

6. Anon.: Engineering Properties of Inconel. Bull. T-7, Development and Res. Div., The International Nickel Co., Inc., March 1943.

TABLE I - TAIL-PIPE-BURNER PERFORMANCE DATA

Run	Altitude (ft)	Flight Mach number M_0	Tunnel static pressure p_s (lb/sq ft abs.)	Free-stream static pressure p_0 (lb/sq ft abs.)	Engine-inlet total pressure P_1 (lb/sq ft abs.)	Engine inlet total temperature T_1 (°R)	Air flow W_a (lb/sec)	Engine fuel flow $W_{f,e}$ (lb/hr)	Tail-pipe fuel flow $W_{f,t}$ (lb/hr)	Total fuel-air ratio f/a	Tail-pipe fuel-air ratio $(f/a)_t$	Jet thrust F_j (lb)	Net thrust F_n (lb)
1	15,000	0.195	1197	(a)	1231	466	57.74	3750	6000	0.0469	0.0396	4454	4070
2	15,000	.200	1180	(a)	1222	474	56.19	3600	5300	.0440	.0357	4221	3837
3	15,000	.230	1183	(a)	1229	466	57.89	3560	4590	.0391	.0296	4096	3643
4	15,000	.220	1183	(a)	1225	464	57.73	3700	3500	.0346	.0230	3960	3525
5	25,000	.195	778	(a)	799	457	38.05	2400	4800	.0525	.0475	2946	2701
6	25,000	.215	774	(a)	798	446	38.70	2440	4500	.0498	.0438	2950	2685
7	25,000	.210	781	(a)	807	503	36.26	2160	4000	.0471	.0408	2592	2321
8	25,000	.200	781	(a)	803	447	38.75	2450	3700	.0441	.0360	2823	2572
9	25,000	.210	778	(a)	801	446	38.69	2460	3200	.0407	.0313	2700	2440
10	25,000	.200	781	(a)	804	458	38.15	2430	2560	.0363	.0254	2542	2287
11	25,000	.380	799	(a)	883	450	42.64	2800	6650	.0615	.0596	3721	3193
12	25,000	.385	784	(a)	868	455	41.54	2740	5010	.0518	.0462	3477	2955
13	25,000	.400	774	(a)	862	457	41.19	2750	3990	.0454	.0373	3330	2796
14	25,000	.380	781	(a)	863	463	40.73	2640	3520	.0420	.0329	3184	2673
15	25,000	.380	780	(a)	859	462	40.68	2620	3470	.0416	.0324	3139	2638
16	25,000	.591	781	(a)	988	475	46.69	3000	7000	.0594	.0569	4373	3470
17	25,000	.590	785	(a)	991	450	48.06	3075	6500	.0554	.0512	4330	3429
18	25,000	.585	781	(a)	982	456	47.16	3030	6050	.0534	.0487	4241	3359
19	25,000	.595	762	(a)	968	460	46.57	3120	5600	.0520	.0463	4231	3337
20	25,000	.590	781	(a)	986	450	47.83	3120	4830	.0462	.0385	4145	3248
21	25,000	.770	785	(a)	1162	482	54.07	3410	4950	.0429	.0345	4874	3524
22	25,000	.760	778	(a)	1142	482	53.26	3300	4750	.0420	.0334	4654	3339
23	25,000	.770	781	(a)	1155	485	53.60	3310	4475	.0404	.0312	4683	3343
24	25,000	.715	866	(a)	1214	478	56.69	3560	4440	.0392	.0295	4807	3494
25	25,000	.768	780	(a)	1150	489	53.11	3350	4060	.0387	.0289	4531	3202
26	25,000	.755	803	(a)	1171	475	55.01	3460	3800	.0367	.0260	4535	3198
27	25,000	.773	778	(a)	1154	482	53.79	3540	3775	.0378	.0269	4605	3258
28	35,000	.215	496	(a)	513	456	24.34	1610	3400	.0572	.0536	1946	1770
29	35,000	.210	493	(a)	509	452	24.34	1620	3320	.0564	.0524	1884	1715
30	35,000	.210	500	(a)	516	460	24.28	1610	3150	.0544	.0498	1859	1688
31	35,000	.215	494	(a)	511	459	24.27	1570	3140	.0539	.0492	1862	1686
32	35,000	.215	496	(a)	513	456	24.35	1520	2780	.0490	.0429	1769	1593
33	35,000	.210	496	(a)	512	447	24.74	1670	2600	.0480	.0406	1841	1670
34	35,000	.230	493	(a)	512	460	24.18	1620	2525	.0476	.0402	1827	1640
35	35,000	.215	493	(a)	510	450	24.14	1610	2500	.0473	.0398	1853	1680
36	35,000	.220	493	(a)	510	474	23.85	1440	2500	.0459	.0389	1664	1489
37	35,000	.225	493	(a)	511	488	23.67	1380	2300	.0432	.0357	1523	1340
38	35,000	.205	500	(a)	515	461	23.86	1500	2200	.0431	.0347	1645	1482
39	35,000	.215	496	(a)	513	459	24.25	1600	1600	.0366	.0253	1653	1477
40	45,000	.235	303	(a)	315	446	14.91	990	1640	.0490	.0422	1053	937
41	45,000	.205	304	(a)	313	474	14.42	940	1600	.0489	.0423	955	855
42	45,000	.245	303	(a)	316	452	14.87	940	1600	.0475	.0406	1018	898
43	45,000	.295	306	(a)	325	442	16.73	1000	1500	.0415	.0332	1029	869
44	45,000	.190	310	(a)	318	460	14.98	960	1500	.0456	.0379	980	884
45	45,000	.210	310	(a)	320	457	14.84	960	1300	.0423	.0333	948	844
46	45,000	.643	372	308	408	459	19.30	1250	2300	.0511	.0453	1698	1298
47	45,000	.619	373	308	400	458	19.27	1240	2000	.0467	.0394	1565	1180
48	45,000	.869	433	308	504	461	23.87	1600	3400	.0582	.0549	2395	1749
49	45,000	.850	422	308	494	456	23.60	1520	3210	.0557	.0516	2371	1749
50	45,000	.874	433	308	506	462	23.73	1490	3030	.0529	.0480	2356	1711
51	45,000	.849	421	308	493	448	23.76	1560	3000	.0533	.0483	2333	1713
52	45,000	.855	425	308	496	466	23.27	1400	2690	.0488	.0429	2206	1584
53	45,000	.863	429	308	501	452	24.04	1510	2500	.0463	.0391	2222	1583
54	45,000	1.078	491	308	640	480	29.81	1890	4240	.0571	.0537	3255	2270
55	45,000	1.087	498	308	648	477	29.89	1960	3900	.0544	.0499	3307	2315
56	45,000	1.088	498	308	649	486	30.25	1900	3560	.0501	.0443	3134	2120
57	45,000	1.083	500	308	643	487	29.84	1760	3240	.0466	.0400	3010	2015
58	45,000	1.075	495	308	637	480	29.18	1890	3200	.0485	.0417	3007	2045
59	45,000	1.300	620	308	850	542	36.59	2200	4600	.0516	.0466	4151	2665
60	45,000	1.312	627	308	865	549	37.15	2180	4200	.0477	.0416	3941	2412
61	45,000	1.310	627	308	863	528	38.16	2210	3950	.0449	.0379	4123	2584
62	45,000	1.310	630	308	863	523	38.26	2340	3400	.0417	.0331	4018	2481
63	45,000	1.512	769	308	1132	575	47.09	2740	5740	.0501	.0447	5729	3536
64	45,000	1.521	785	308	1145	564	48.38	2840	5500	.0479	.0418	5724	3485
65	45,000	1.514	774	308	1135	566	47.90	2700	4900	.0441	.0371	5479	3264

[a] $p_0 = p_s$.

OBTAINED WITH VARIABLE-AREA EXHAUST NOZZLE

Augmented thrust ratio $F_n/F_{n,e}$	Specific fuel consumption W_f/F_n (lb/(hr) (lb thrust)	Turbine-outlet total pressure P_6 (lb/sq ft abs.)	Turbine-outlet total temperature T_6 (°R)	Combustion-chamber-inlet static pressure p_7 (lb/sq ft abs.)	Combustion-chamber inlet velocity V_7 (ft/sec)	Exhaust-nozzle total pressure P_8 (lb/sq ft abs.)	Exhaust-gas total temperature T_j (°R)	Tail-pipe combustion efficiency η_b	Run
1.306	2.396	2445	1756	2327	468	2269	3004	0.787	1
1.315	2.320	2366	1712	2254	456	2201	2960	.827	2
1.245	2.237	2355	1686	2237	464	2195	2652	.766	3
1.162	2.043	2420	1721	2304	457	2265	2408	.699	4
1.349	2.666	1578	1686	1496	462	1449	3073	.717	5
1.332	2.585	1560	1689	1469	478	1424	3040	.754	6
1.337	2.654	1463	1667	1379	469	1331	3030	.790	7
1.276	2.391	1564	1676	1477	470	1440	2810	.742	8
1.202	2.320	1570	1700	1483	472	1450	2556	.650	9
1.127	2.182	1594	1701	1513	455	1498	2257	.513	10
1.480	2.960	1778	1706	1686	469	1617	3435	.741	11
1.390	2.623	1746	1738	1657	469	1607	3180	.782	12
1.329	2.411	1734	1748	1646	468	1608	2957	.795	13
1.293	2.305	1738	1725	1652	454	1621	2784	.770	14
1.290	2.309	1698	1728	1612	465	1581	2794	.789	15
1.543	2.882	1943	1737	1841	477	1776	3512	.804	16
1.475	2.792	1966	1710	1864	476	1795	3262	.762	17
1.462	2.703	1954	1726	1852	474	1787	3264	.799	18
1.447	2.613	1957	1748	1858	472	1803	3239	.805	19
1.407	2.448	1973	1719	1868	471	1820	3032	.828	20
1.408	2.372	2243	1717	2131	465	2083	3004	.888	21
1.385	2.546	2169	1692	2057	468	2003	2900	.849	22
1.378	2.329	2200	1693	2089	463	2046	2863	.871	23
1.331	2.290	2341	1715	2226	465	2190	2773	.845	24
1.293	2.314	2259	1721	2156	452	2115	2691	.789	25
1.268	2.270	2257	1690	2144	460	2117	2563	.759	26
1.265	2.245	2309	1747	2204	453	2179	2666	.801	27
1.377	2.831	1000	1749	947	486	909	3309	.749	28
1.316	2.880	1008	1742	951	481	916	3052	.639	29
1.306	2.820	1009	1760	955	483	921	3038	.659	30
1.332	2.794	987	1736	934	486	899	3104	.705	31
1.295	2.699	967	1707	913	489	881	2917	.699	32
1.255	2.557	1015	1757	957	487	928	2844	.665	33
1.286	2.527	1005	1754	952	478	924	2929	.722	34
1.318	2.446	1000	1737	945	475	917	3054	.812	35
1.288	2.646	932	1672	871	488	843	2880	.738	36
1.202	2.746	912	1667	852	493	825	2558	.595	37
1.232	2.497	968	1685	914	469	888	2660	.661	38
1.142	2.167	1010	1752	956	471	945	2386	.606	39
1.222	2.807	599	1749	557	500	540	2748	.597	40
1.178	2.971	575	1754	535	505	516	2610	.509	41
1.228	2.829	584	1710	543	500	526	2698	.600	42
1.065	2.877	599	1731	557	551	545	2128	.362	43
1.141	2.783	598	1744	557	500	543	2442	.472	44
1.116	2.678	598	1741	553	495	545	2329	.444	45
1.415	2.735	776	1740	730	494	701	3068	.733	46
1.300	2.746	769	1738	718	498	694	2662	.587	47
1.513	2.859	979	1741	925	486	889	3161	.660	48
1.537	2.704	950	1742	896	495	860	3273	.760	49
1.550	2.642	958	1699	908	478	867	3179	.764	50
1.480	2.662	961	1735	905	490	872	3110	.718	51
1.500	2.582	917	1679	865	484	826	3036	.771	52
1.391	2.533	960	1703	906	483	873	2789	.679	53
1.607	2.700	1205	1718	1140	486	1090	3242	.716	54
1.605	2.531	1240	1730	1172	476	1128	3285	.779	55
1.470	2.575	1228	1732	1164	484	1118	2928	.672	56
1.492	2.481	1169	1676	1109	483	1065	2867	.716	57
1.473	2.489	1209	1720	1142	471	1103	2929	.697	58
1.628	2.552	1474	1726	1387	489	1333	3108	.724	59
1.472	2.645	1474	1712	1385	492	1336	2734	.593	60
1.501	2.384	1513	1704	1423	488	1377	2826	.709	61
1.409	2.314	1541	1721	1452	483	1416	2656	.665	62
1.717	2.398	1890	1711	1784	485	1721	3156	.770	63
1.620	2.393	1943	1708	1835	483	1771	2970	.717	64
1.603	2.328	1877	1663	1779	478	1723	2832	.719	65

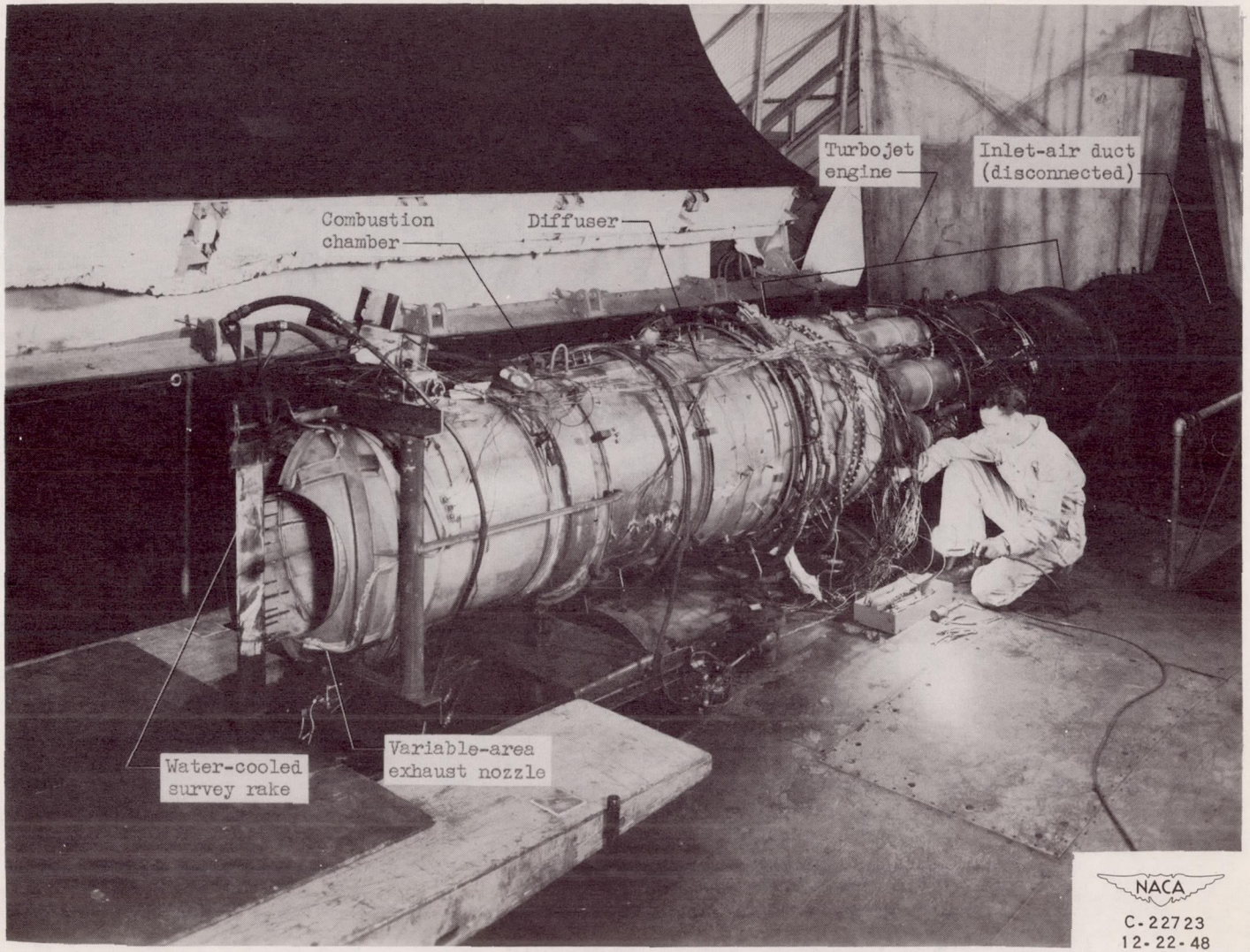

Figure 1. - Altitude-wind-tunnel installation of turbojet engine with 32-inch-diameter tail-pipe burner and variable-area exhaust nozzle.

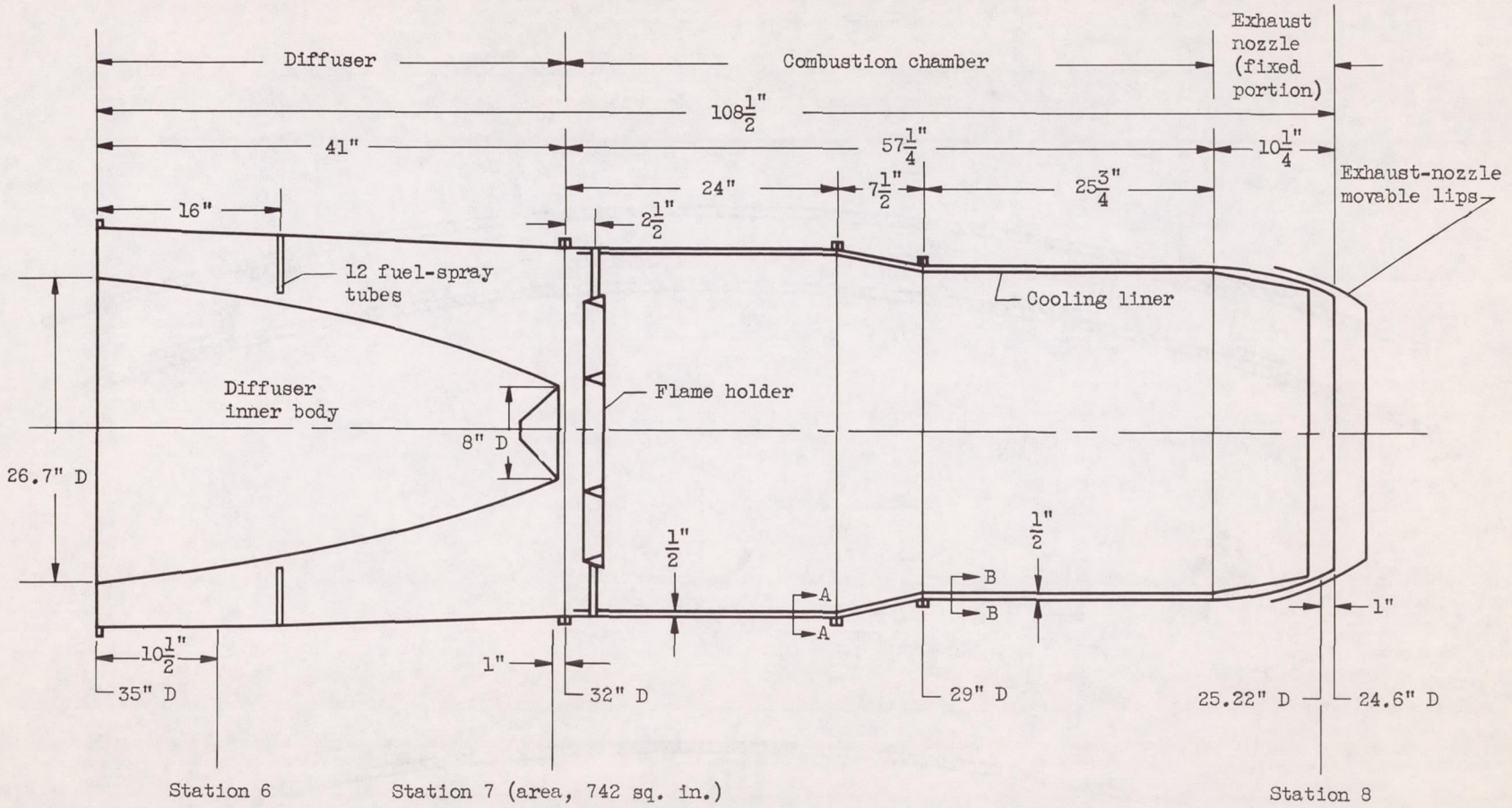

(a) Cross section showing stations at which instrumentation was installed.

Figure 2. - Tail-pipe burner assembly.

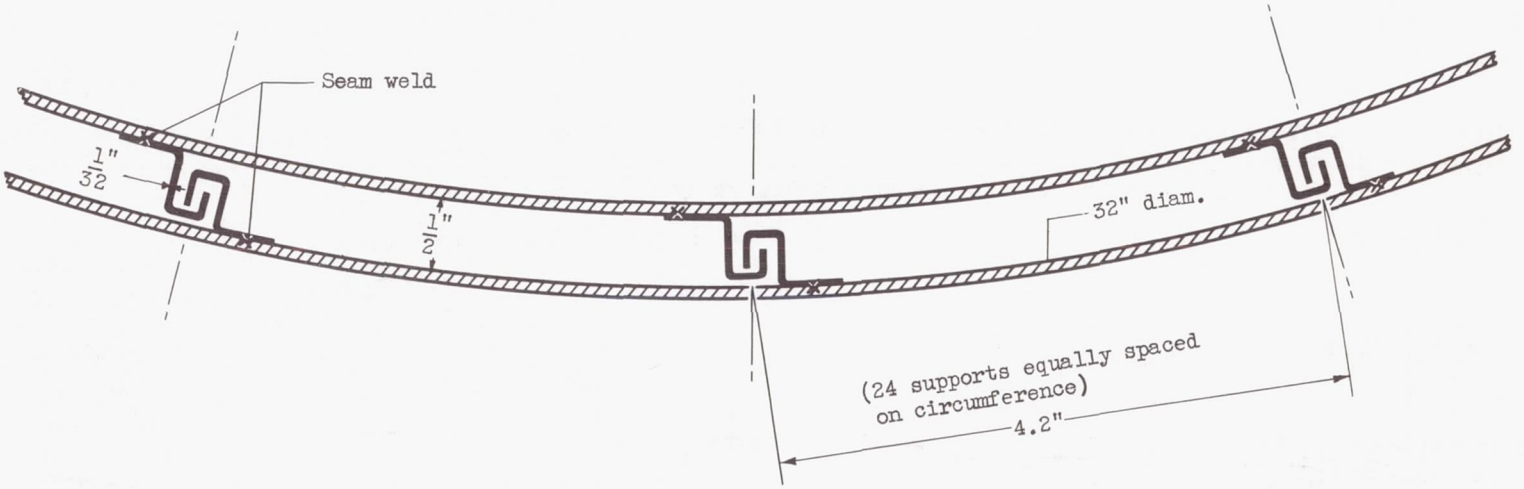

Section A-A, interlocking channels

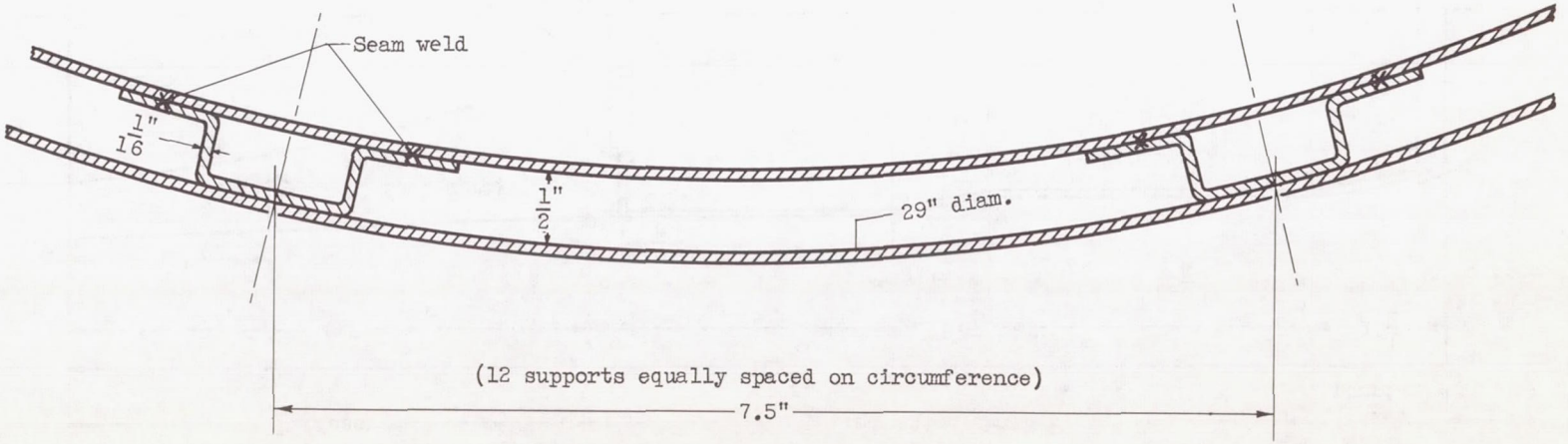

Section B-B, hat-section stiffeners

(b) Details of cooling-liner supports.

Figure 2. - Concluded. Tail-pipe-burner assembly.

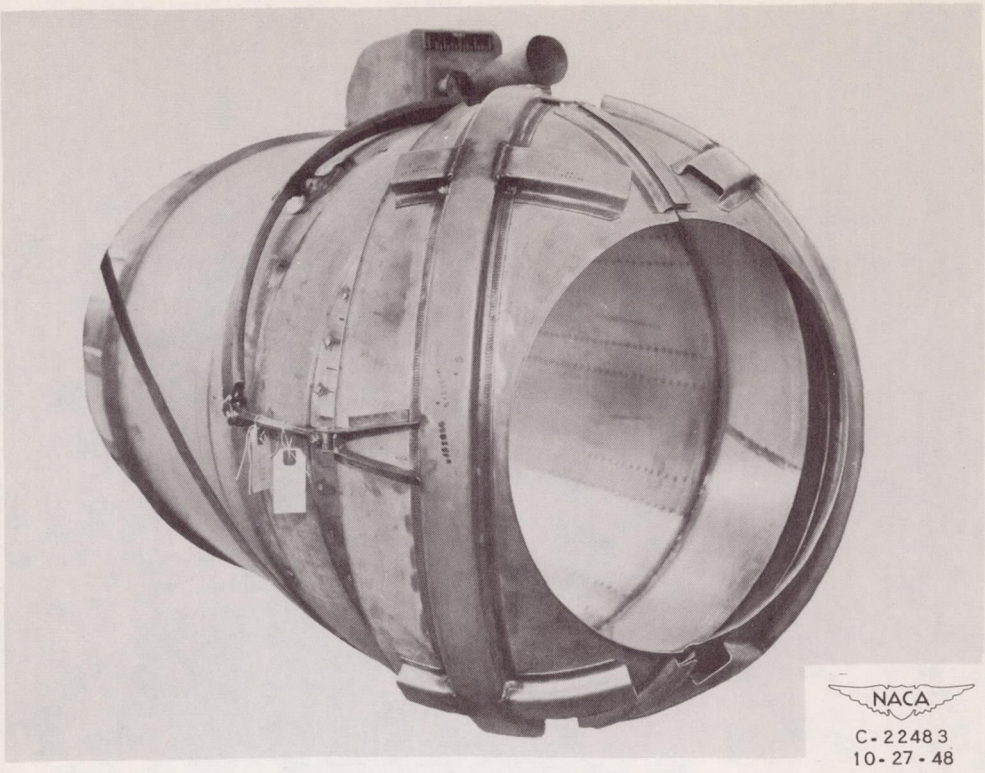

(a) Closed position.

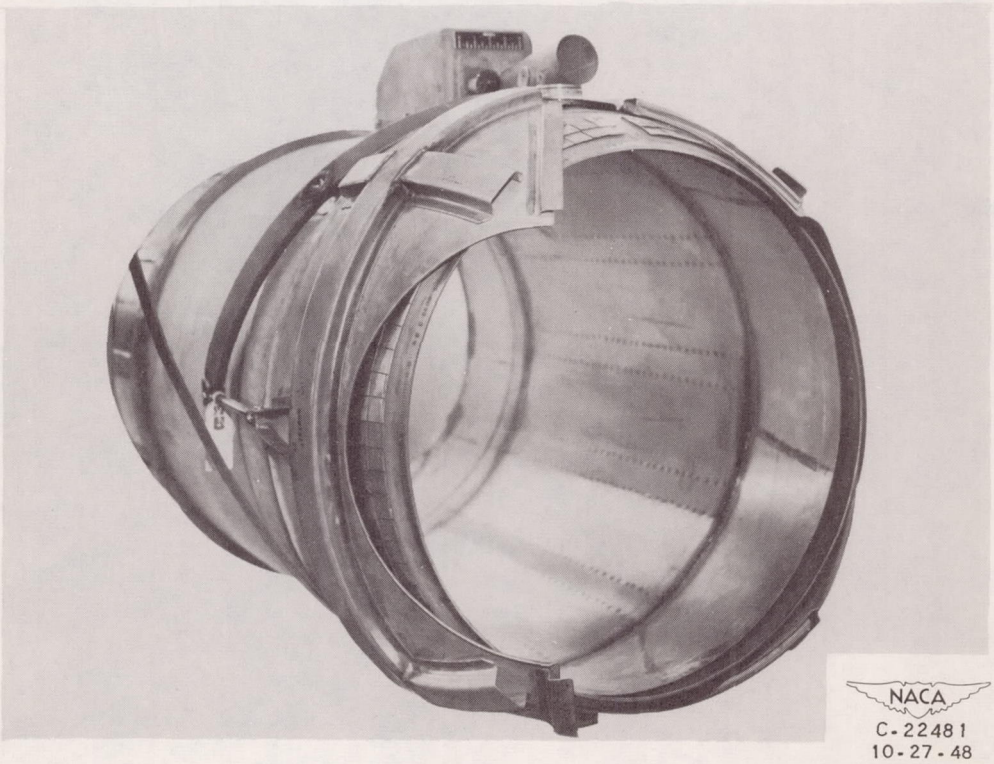

(b) Full-open position.

Figure 3. - Variable-area exhaust nozzle.

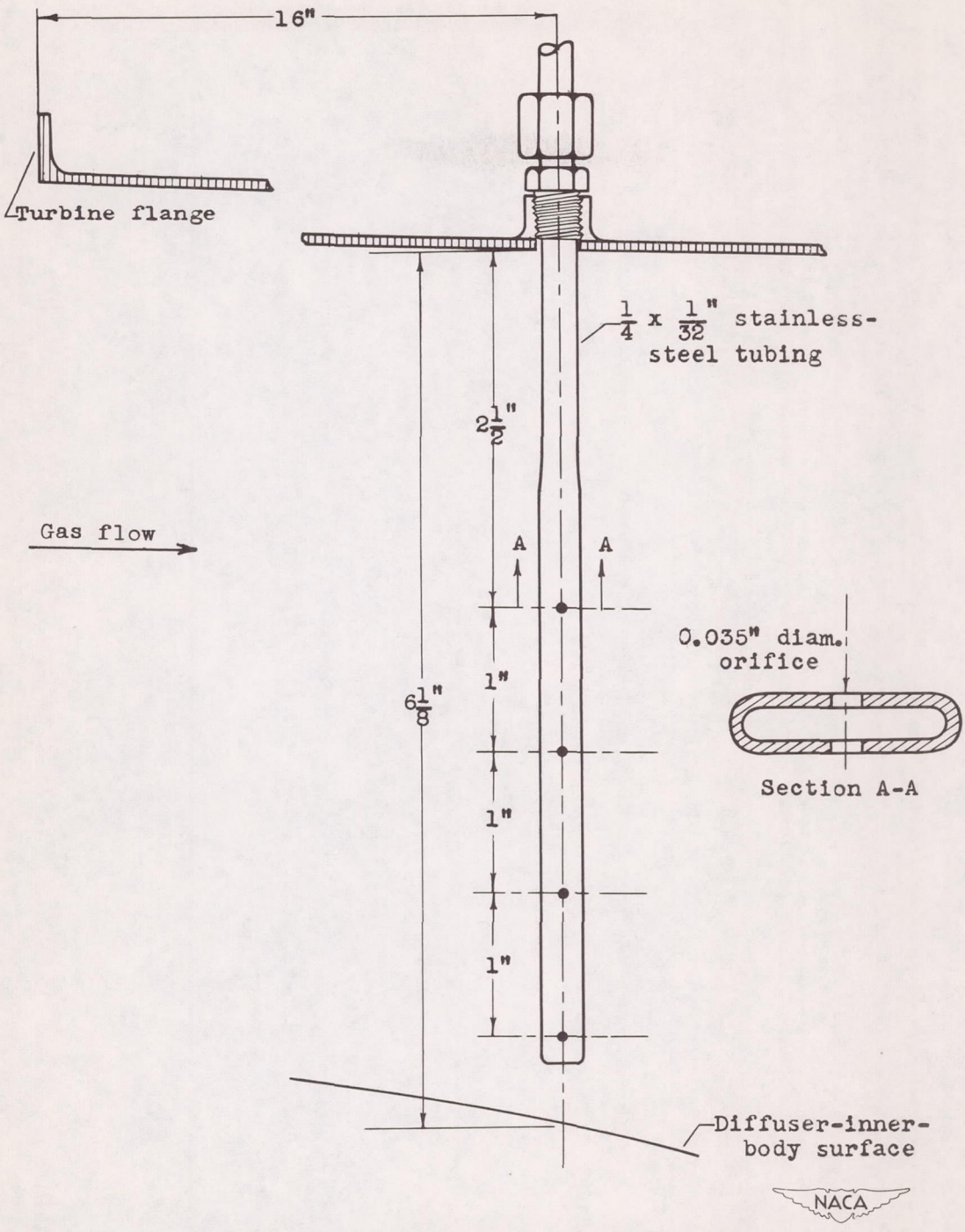

Figure 4. - Details of fuel-spray tubes.

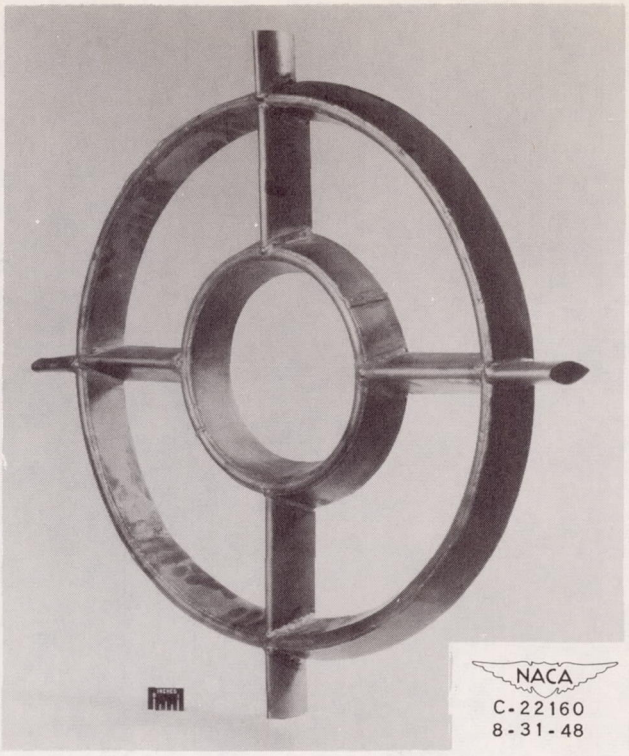

(a) Upstream face.

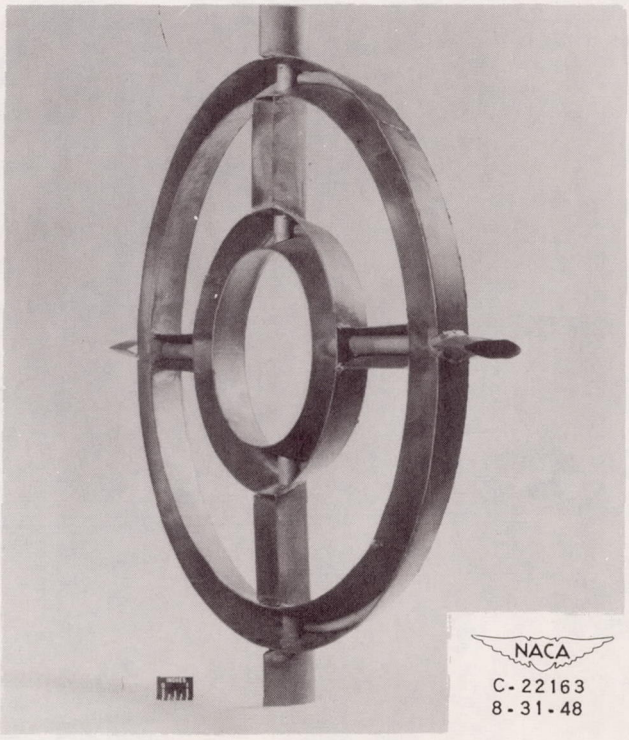

(b) Downstream face.

Figure 5. - Two-annular-V flame holder.

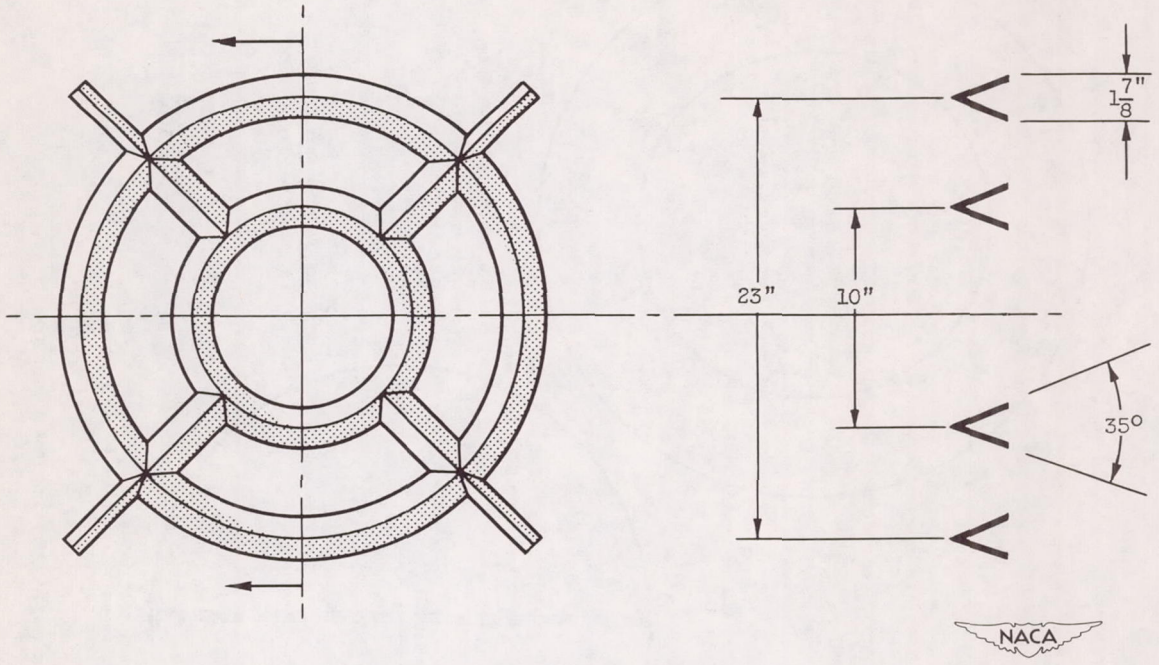

(c) Schematic diagram.

Figure 5. - Concluded. Two-annular-V flame holder.

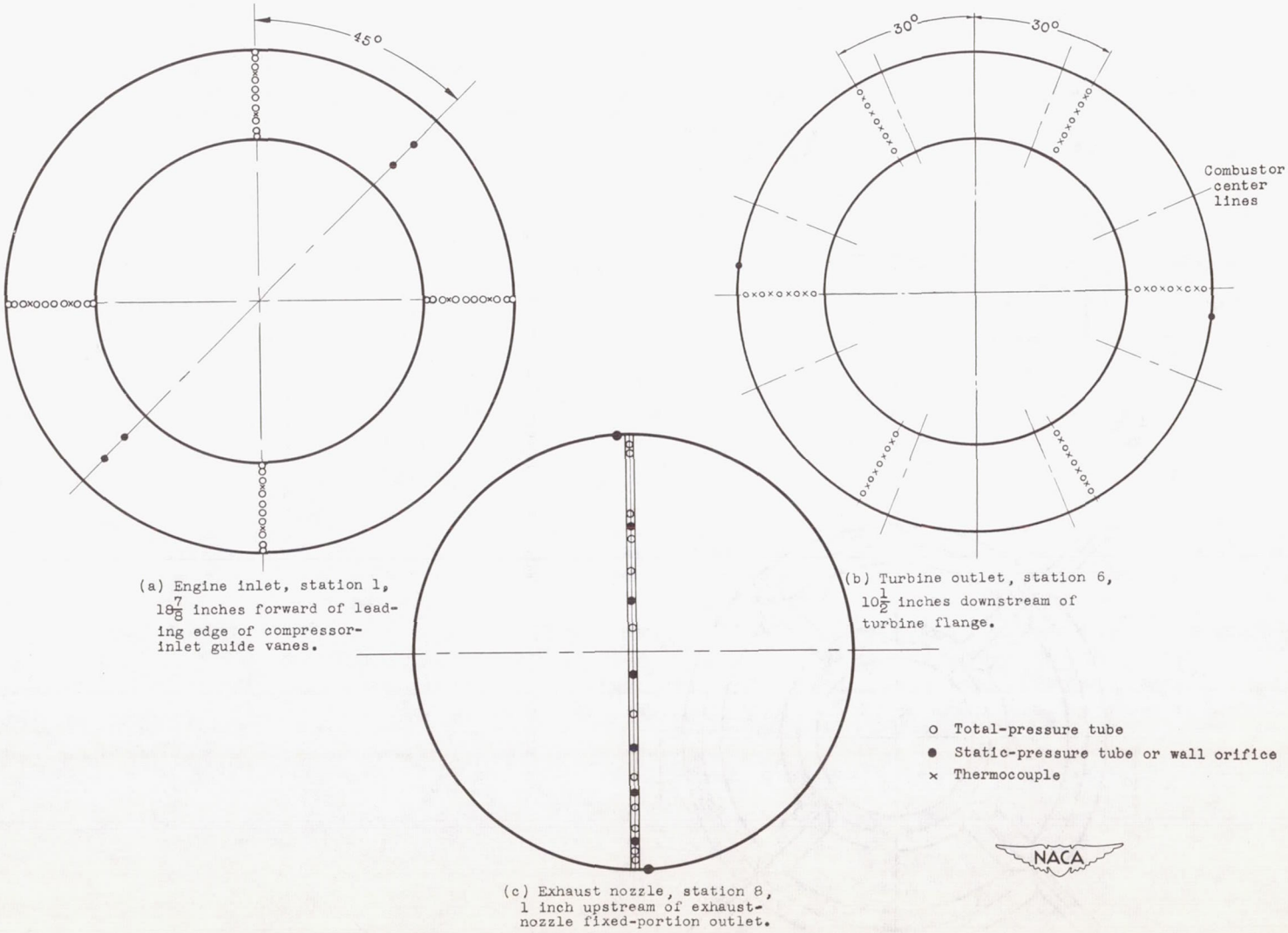

(a) Engine inlet, station 1, $18\frac{7}{8}$ inches forward of leading edge of compressor-inlet guide vanes.

(b) Turbine outlet, station 6, $10\frac{1}{2}$ inches downstream of turbine flange.

(c) Exhaust nozzle, station 8, 1 inch upstream of exhaust-nozzle fixed-portion outlet.

Figure 6. - Cross sections of measuring stations showing location of instrumentation.

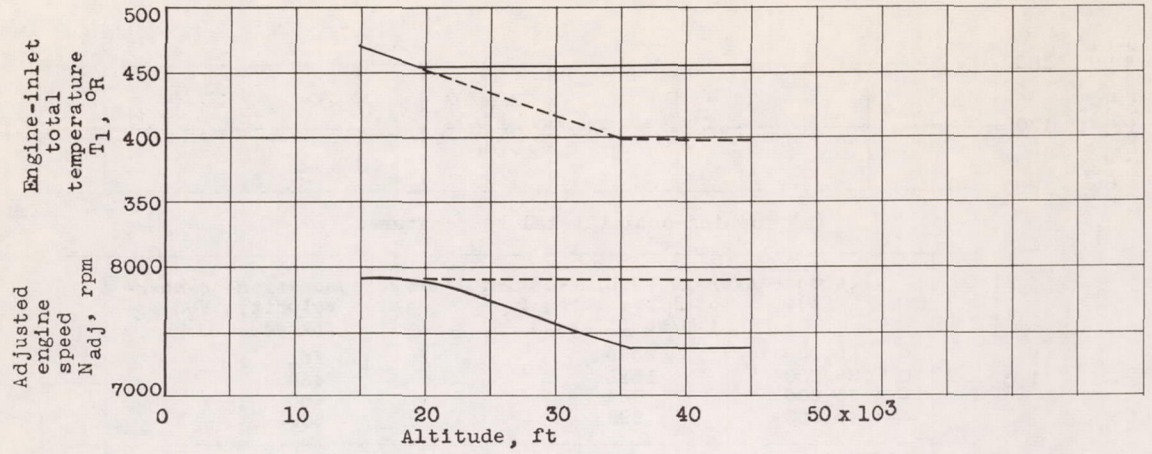

(a) Flight Mach number, 0.22.

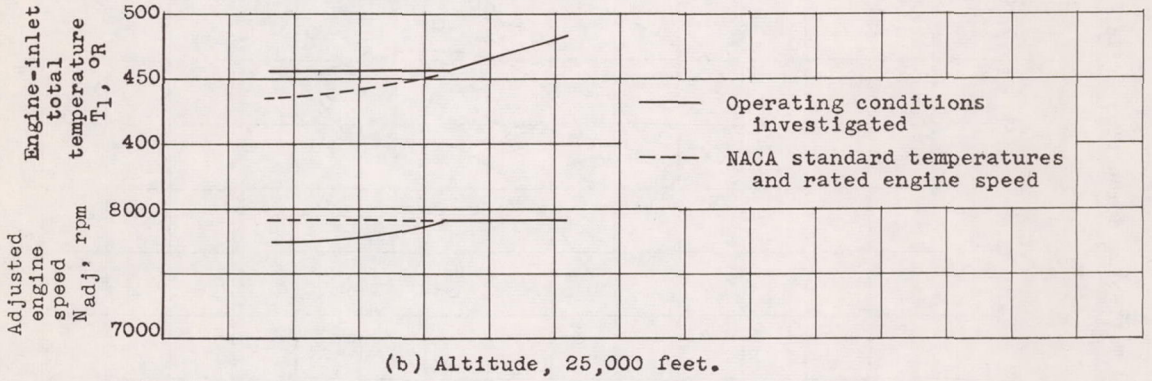

(b) Altitude, 25,000 feet.

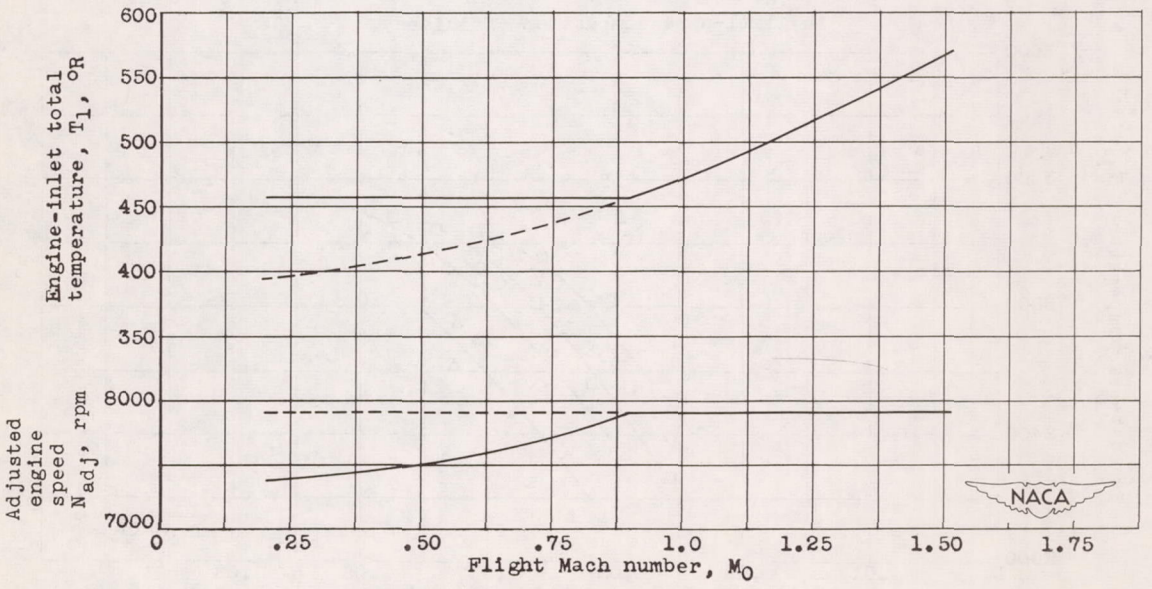

(c) Altitude, 45,000 feet.

Figure 7. - Average values of engine-inlet temperature and equivalent engine speed at which investigation was conducted. Actual engine speed, 7900 rpm; average turbine-outlet temperature, 1710° R.

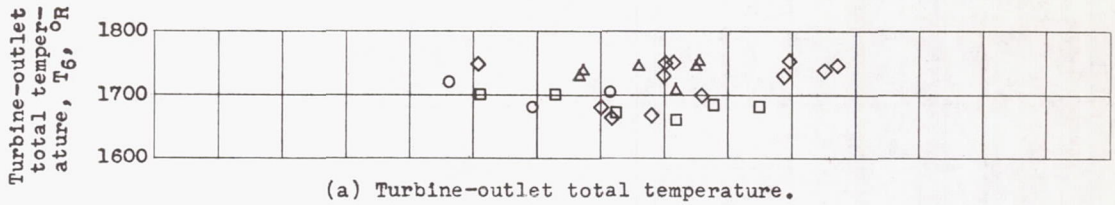

(a) Turbine-outlet total temperature.

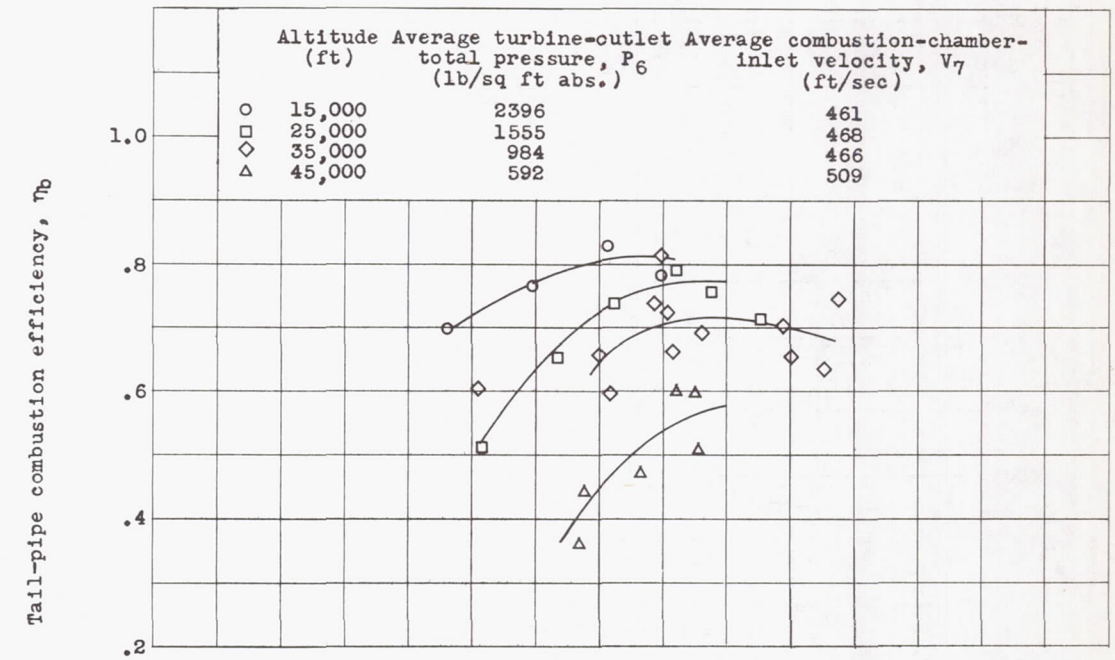

(b) Tail-pipe combustion efficiency.

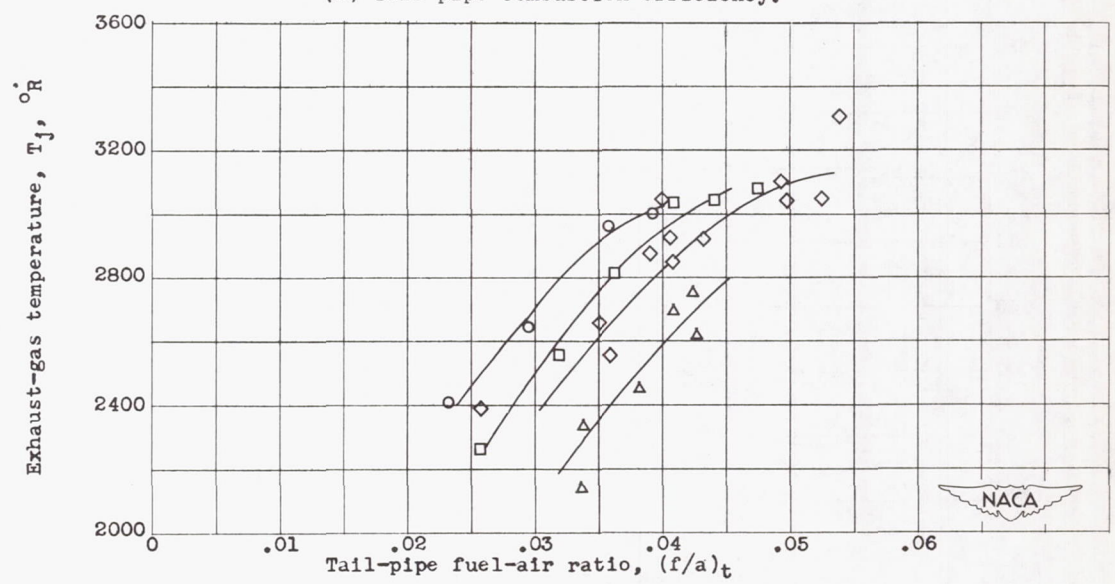

(c) Exhaust-gas total temperature

Figure 8. - Effect of altitude on variation of performance with tail-pipe fuel-air ratio. Flight Mach number, 0.22; engine speed, 7900 rpm.

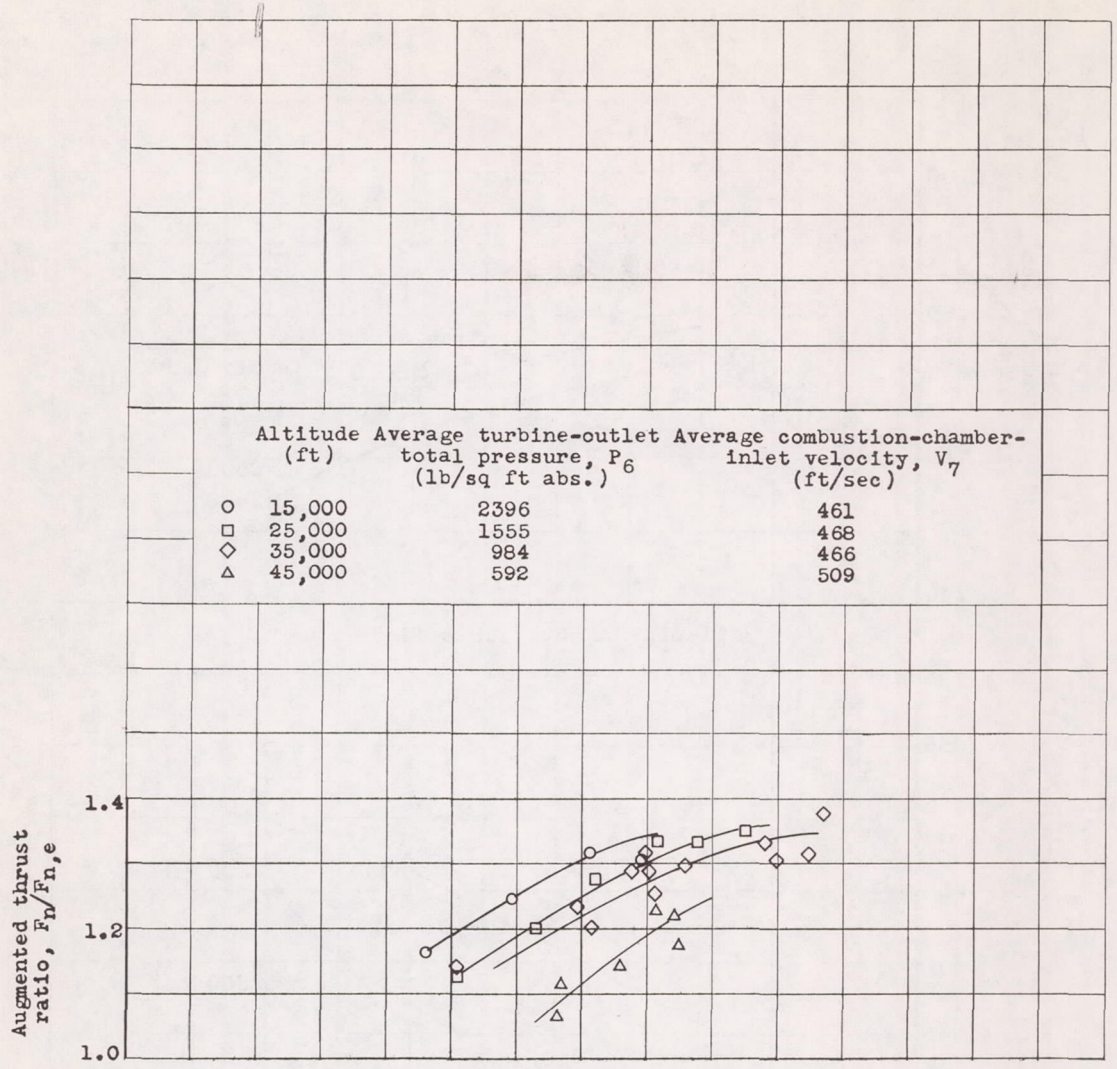

(d) Augmented thrust ratio.

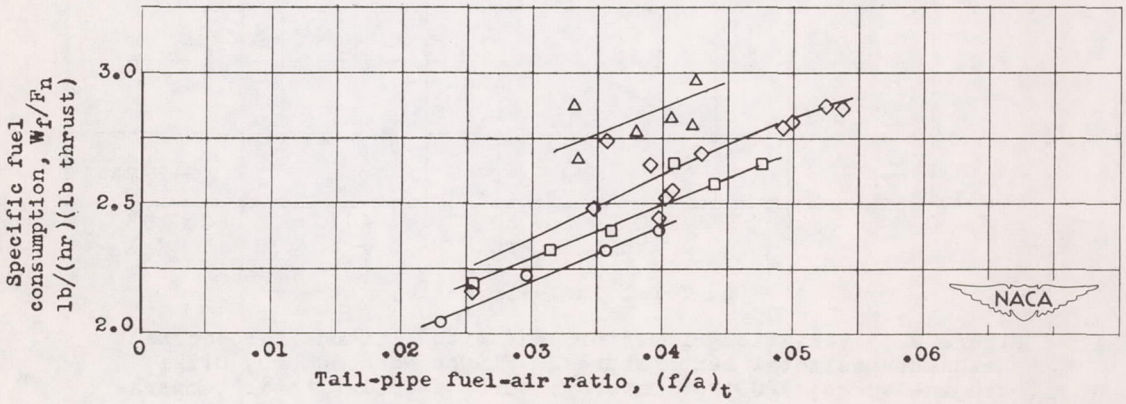

(e) Specific fuel consumption.

Figure 8. - Concluded. Effect of altitude on variation of performance with tail-pipe fuel-air ratio. Flight Mach number, 0.22; engine speed, 7900 rpm.

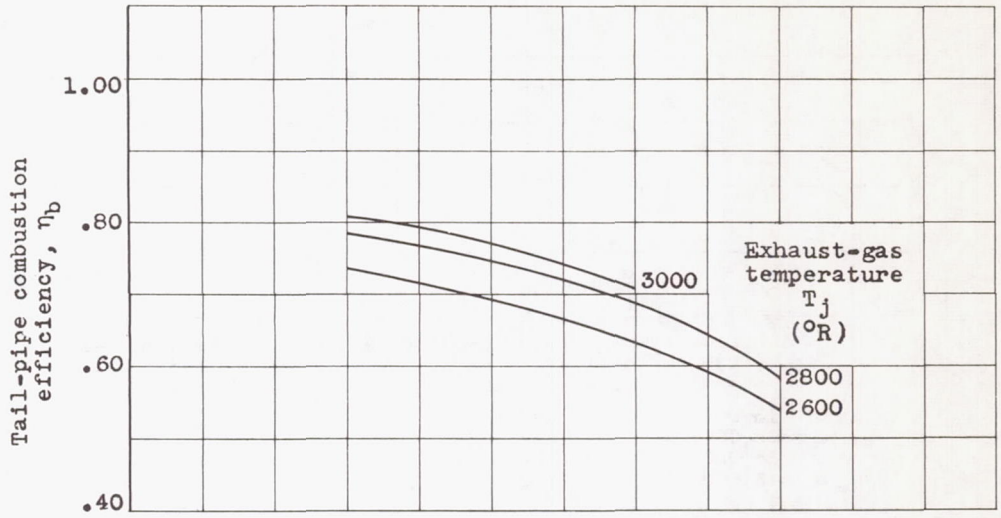

(a) Tail-pipe combustion efficiency.

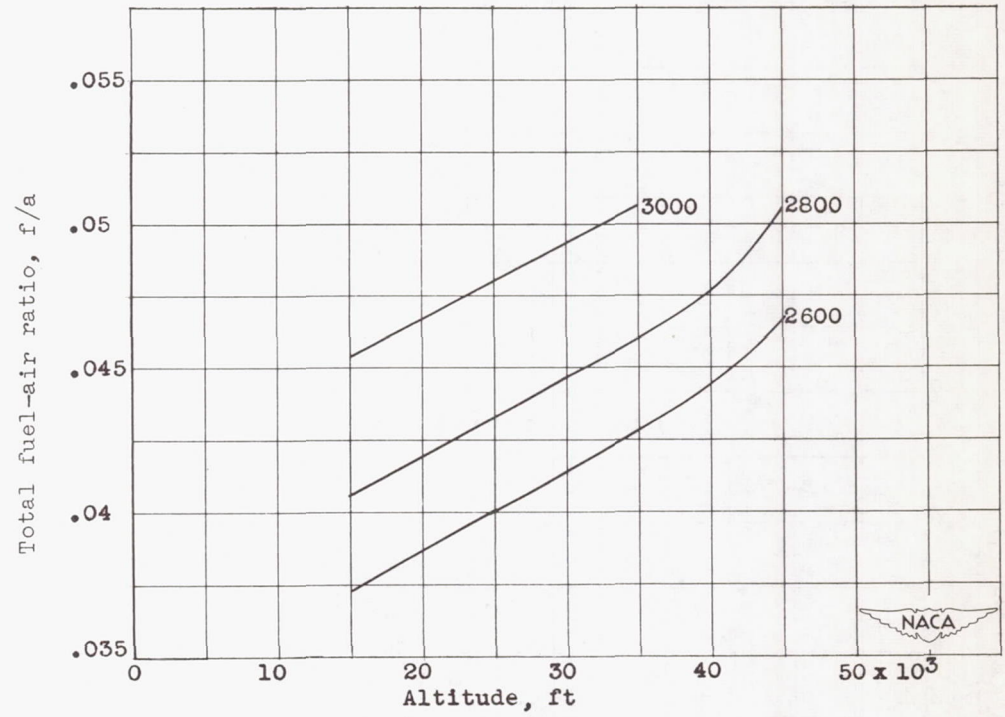

(b) Total fuel-air ratio.

Figure 9. - Variation of performance with altitude for constant exhaust-gas total temperatures. Flight Mach number, 0.22; engine speed, 7900 rpm; average turbine-outlet total temperature, 1710° R.

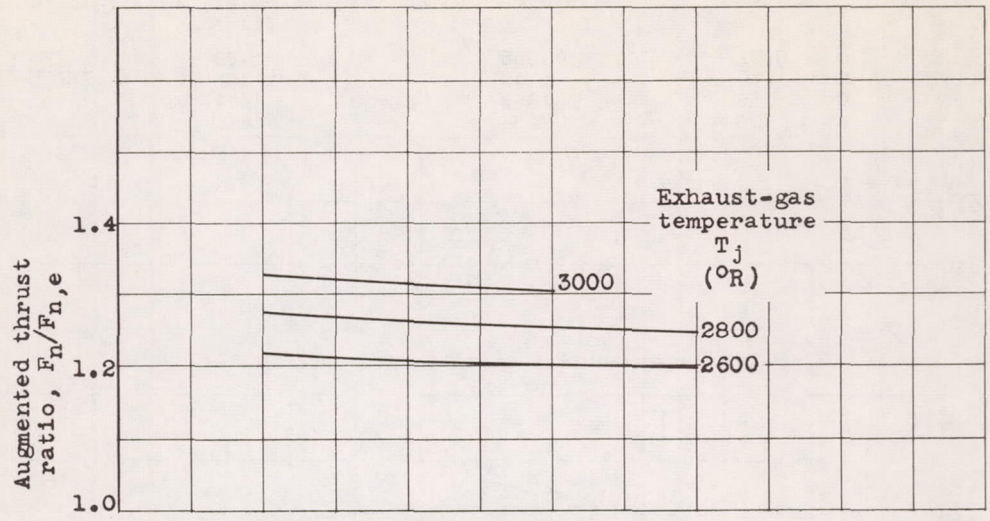

(c) Augmented thrust ratio.

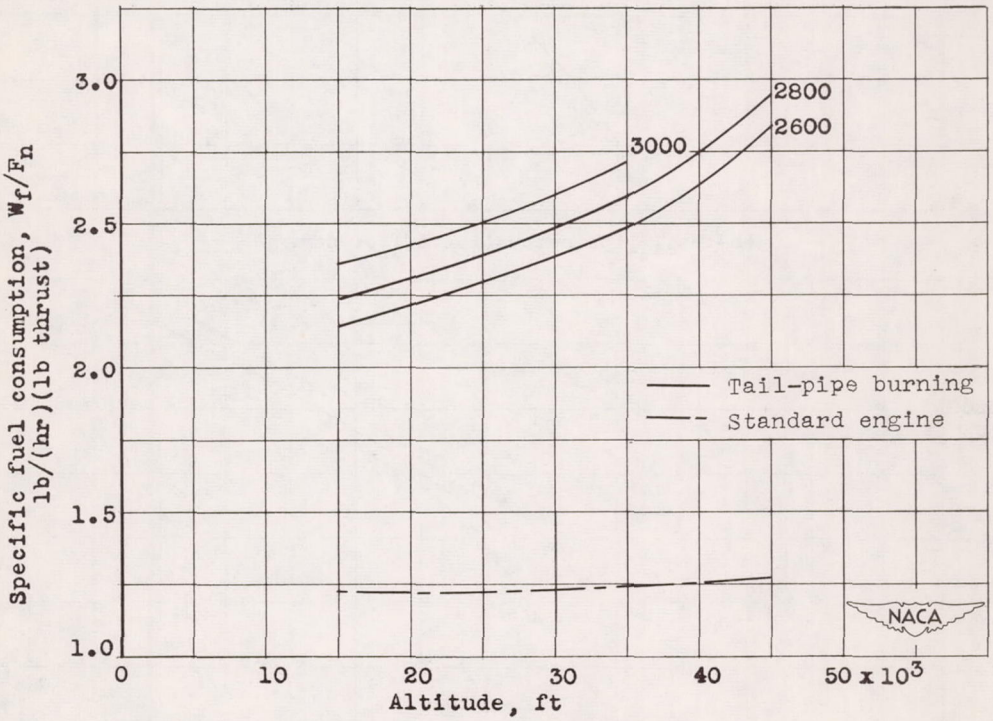

(d) Specific fuel consumption.

Figure 9. - Concluded. Variation of performance with altitude for constant exhaust-gas total temperatures. Flight Mach number, 0.22; engine speed, 7900 rpm; average turbine-outlet temperature, 1710° R.

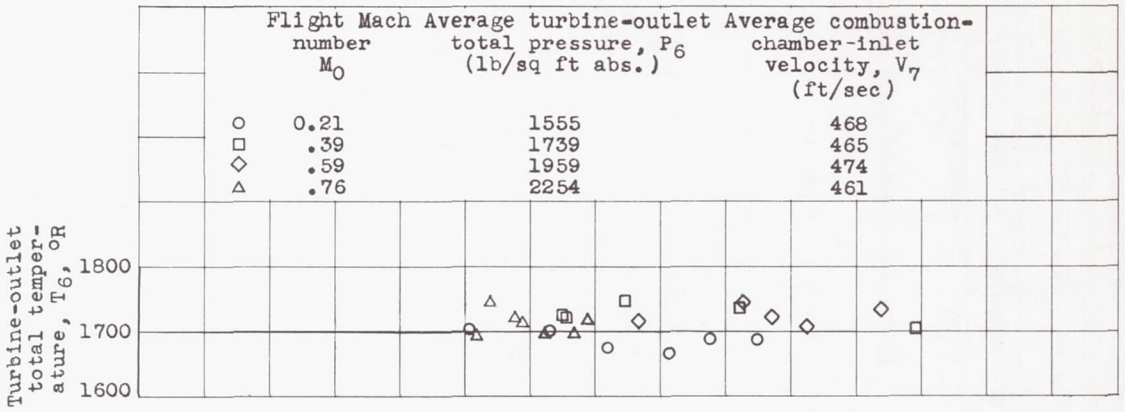

(a) Turbine-outlet total temperature.

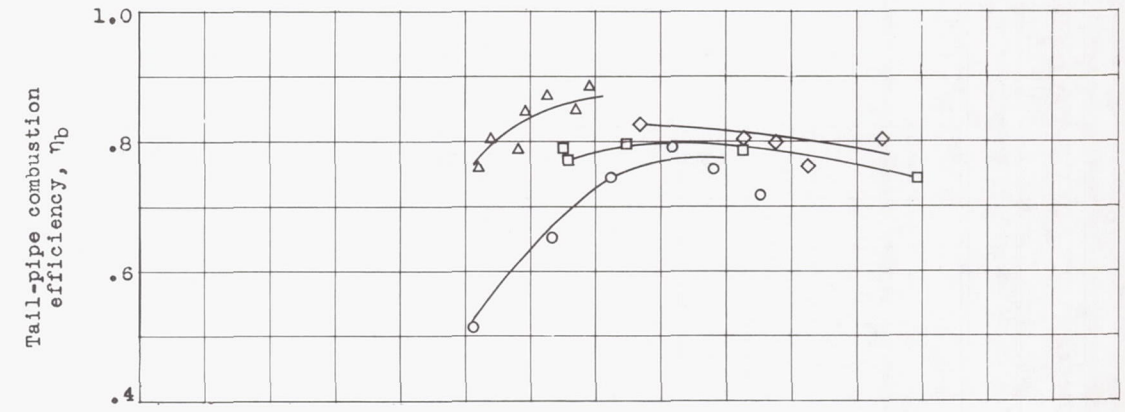

(b) Tail-pipe combustion efficiency.

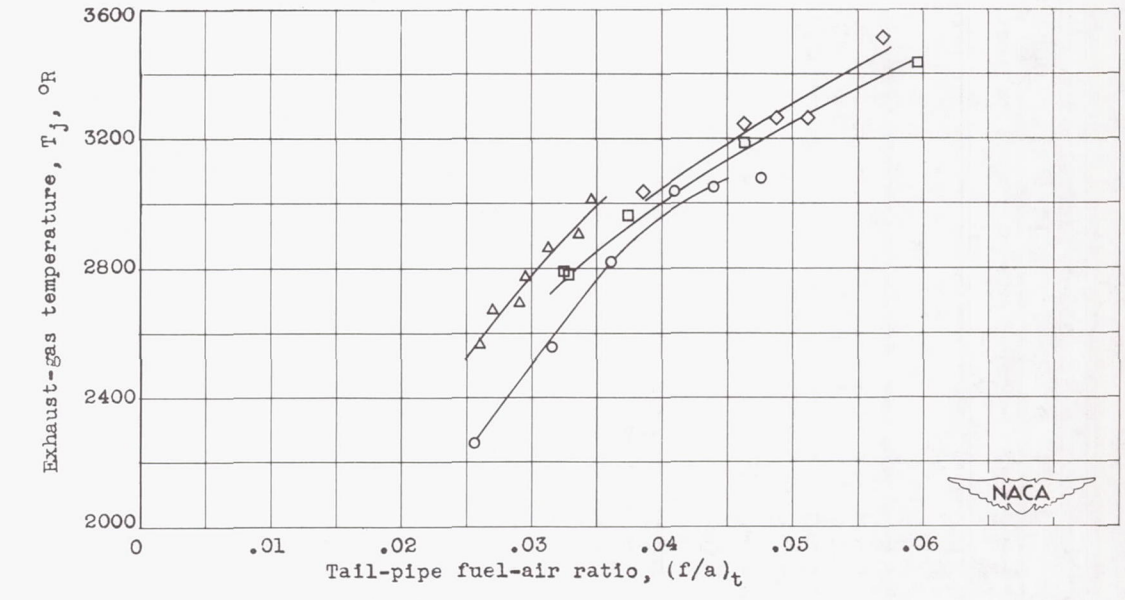

(c) Exhaust-gas total temperature.

Figure 10. - Effect of flight Mach number on variation of performance with tail-pipe fuel-air ratio. Altitude, 25,000 feet; engine speed, 7900 rpm.

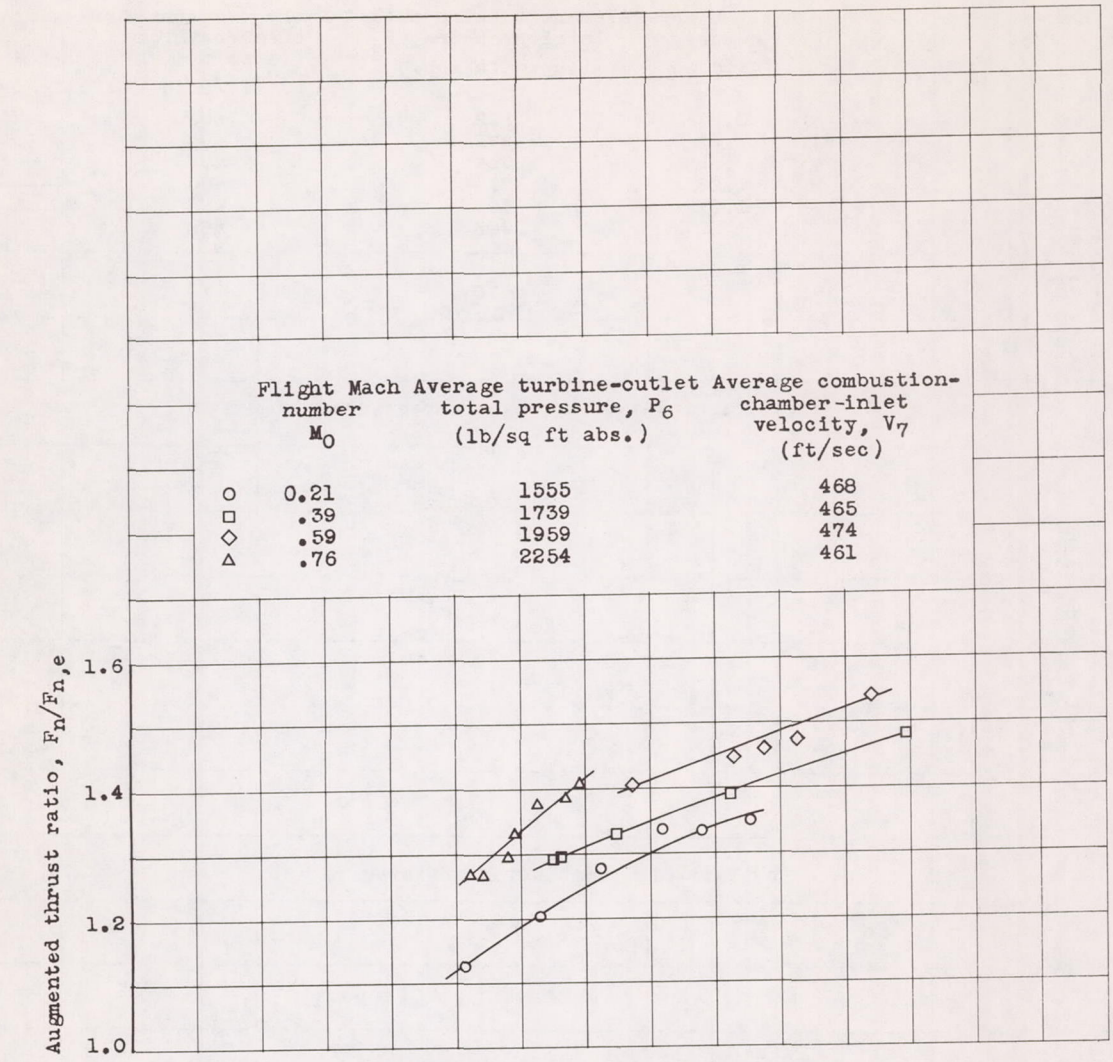

(d) Augmented thrust ratio.

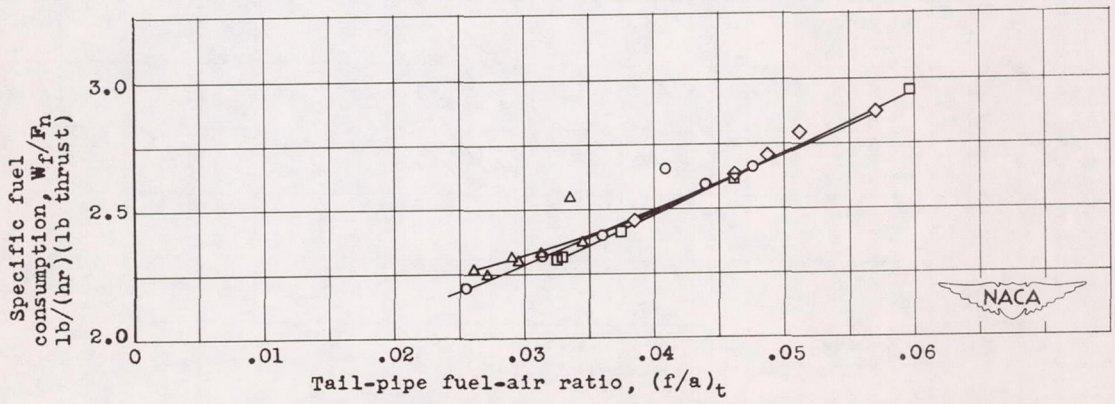

(e) Specific fuel consumption.

Figure 10. - Concluded. Effect of flight Mach number on variation of performance with tail-pipe fuel-air ratio. Altitude, 25,000 feet; engine speed, 7900 rpm.

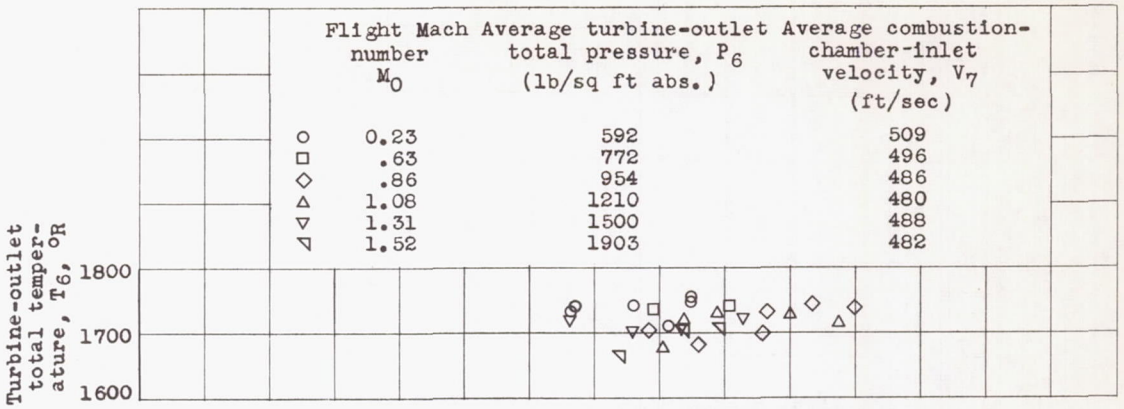

(a) Turbine-outlet total temperature.

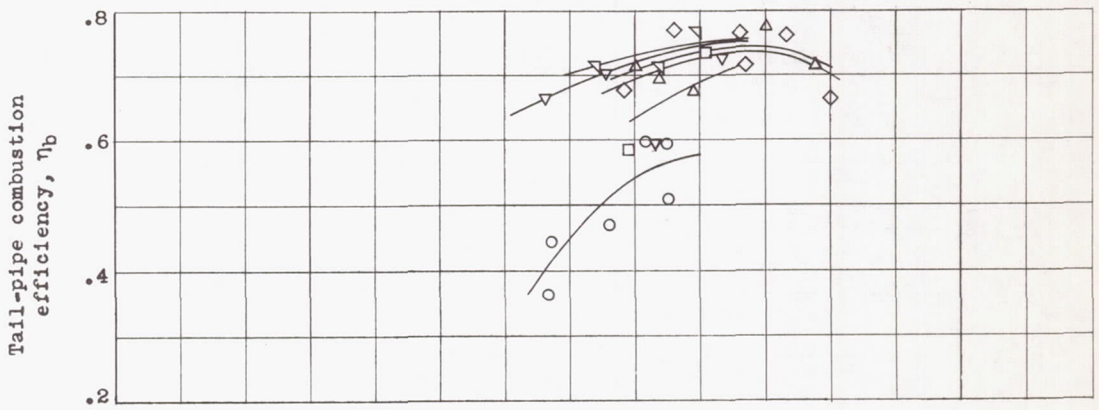

(b) Tail-pipe combustion efficiency.

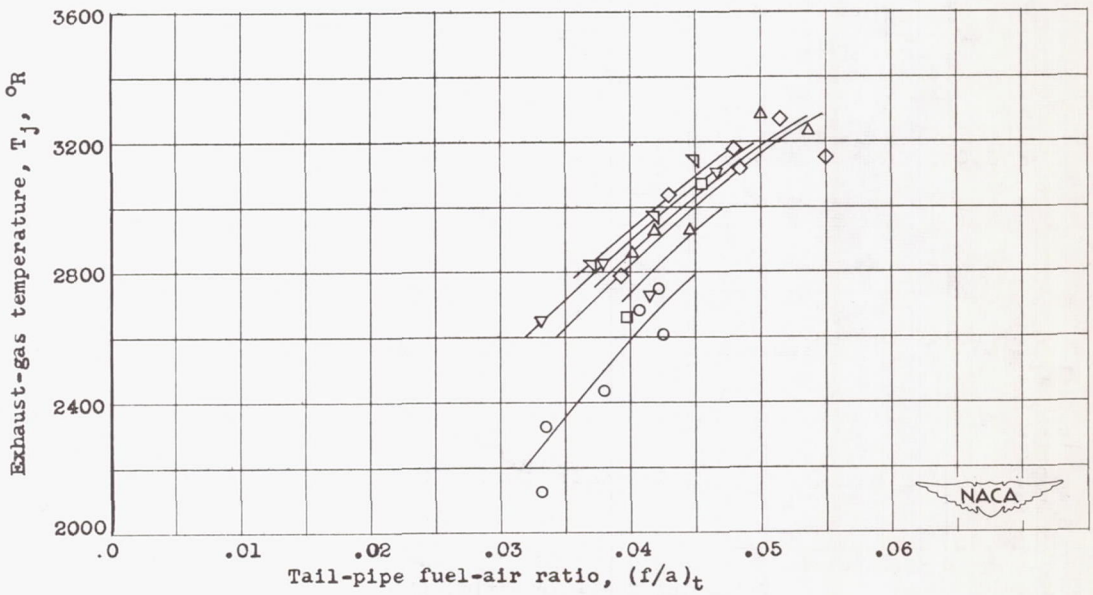

(c) Exhaust-gas total temperature.

Figure 11. - Effect of flight Mach number on variation of performance with tail-pipe fuel-air ratio. Altitude, 45,000 feet; engine speed, 7900 rpm.

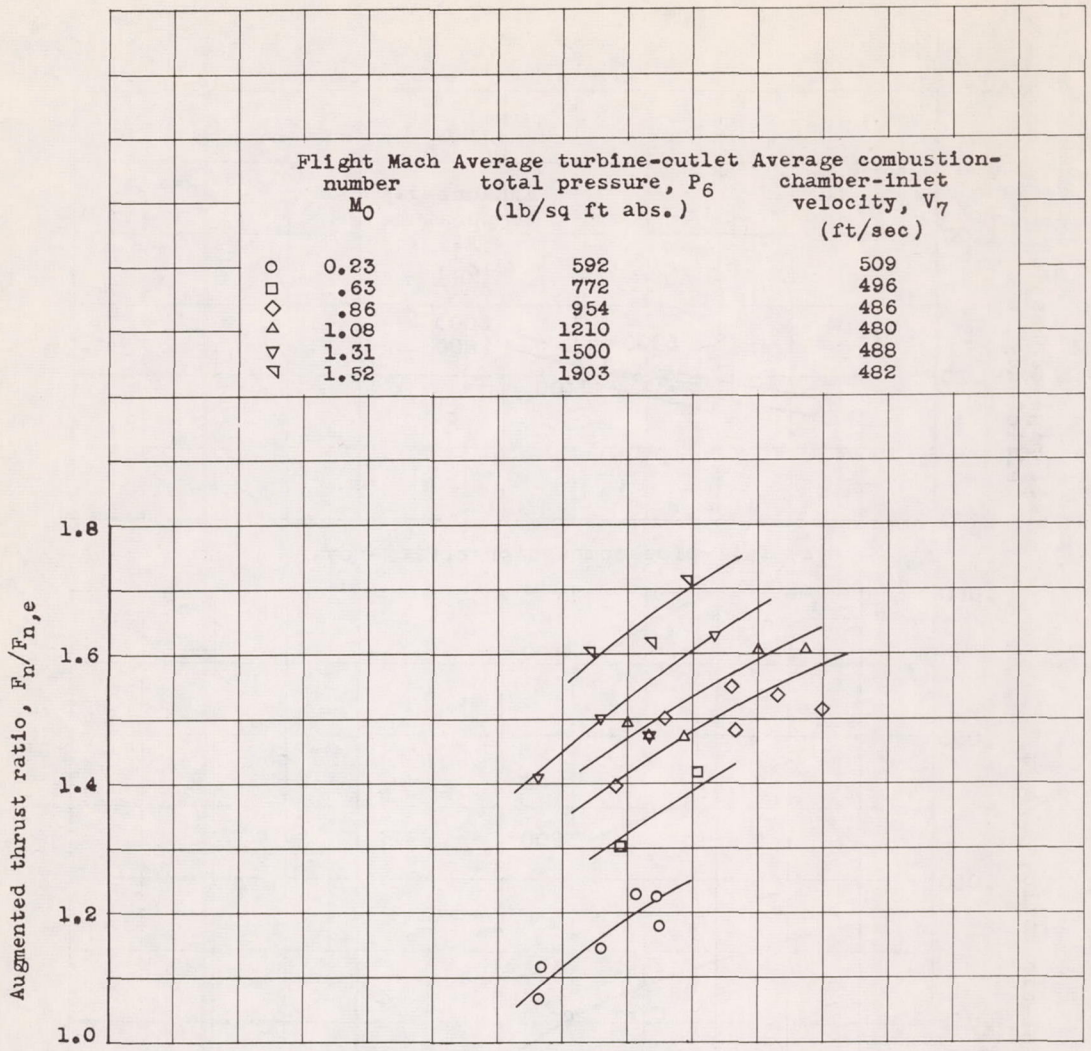

(d) Augmented thrust ratio.

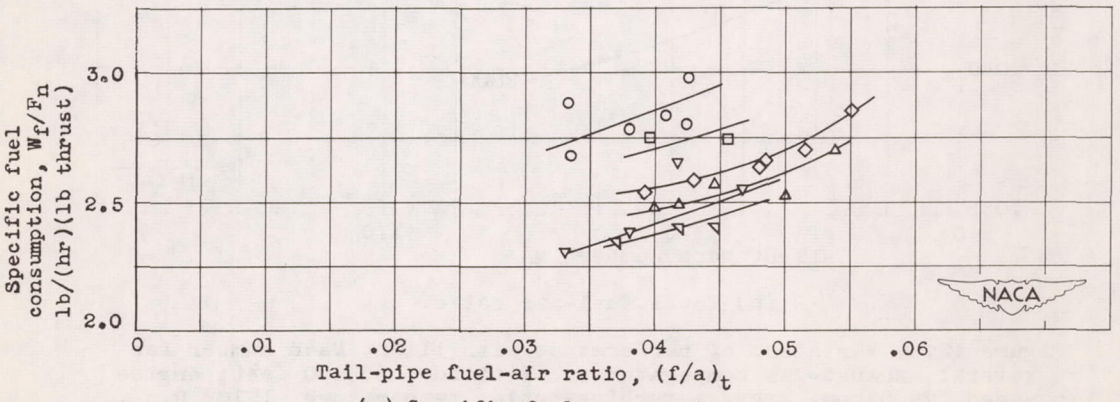

(e) Specific fuel consumption.

Figure 11. - Concluded. Effect of flight Mach number on variation of performance with tail-pipe fuel-air ratio. Altitude, 45,000 feet; engine speed, 7900 rpm.

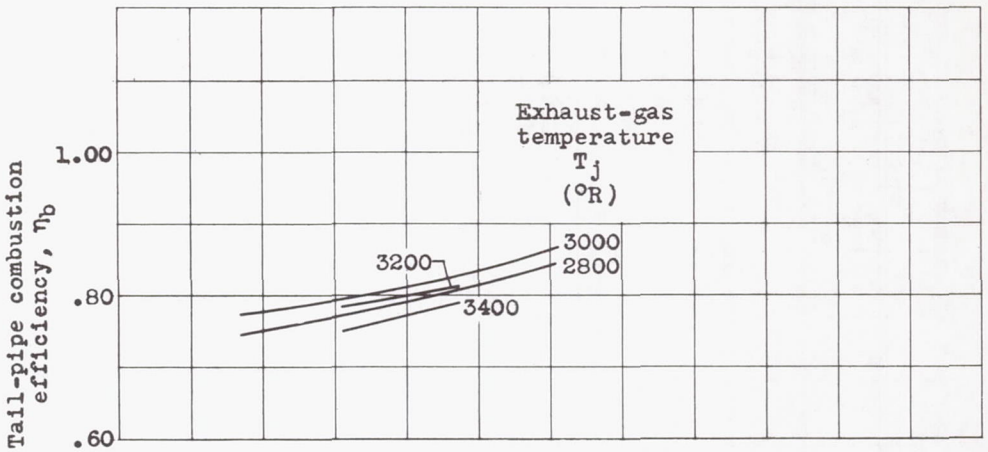

(a) Tail-pipe combustion efficiency.

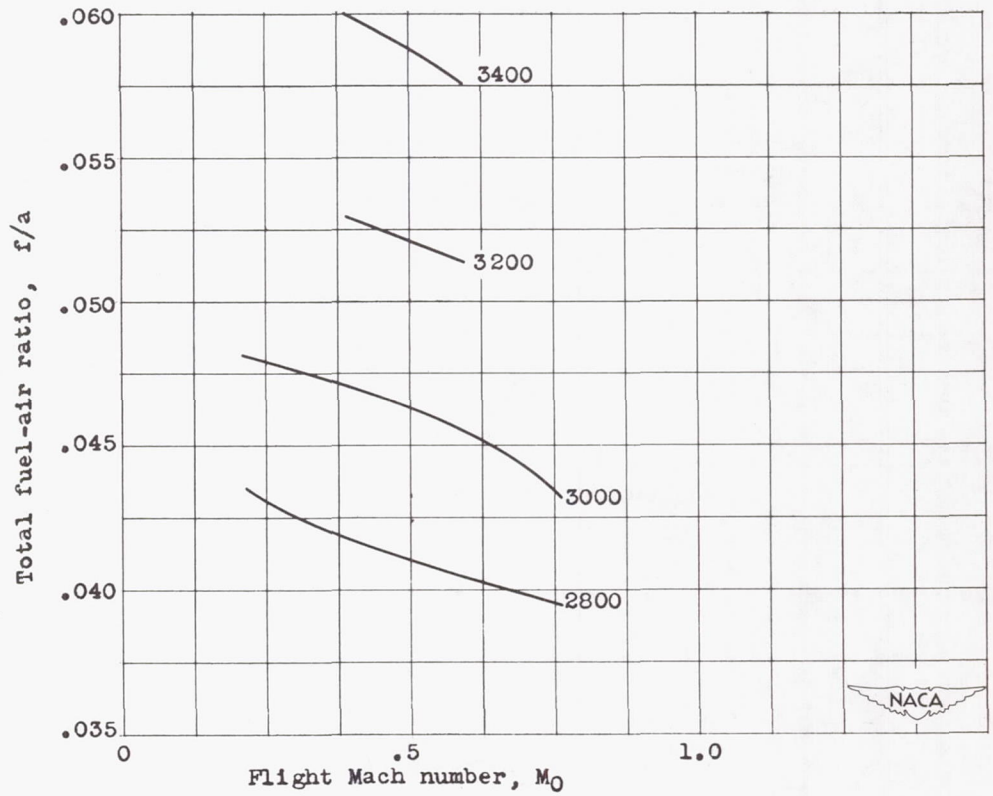

(b) Total fuel-air ratio.

Figure 12. - Variation of performance with flight Mach number for several exhaust-gas temperatures. Altitude, 25,000 feet; engine speed, 7900 rpm; average turbine-outlet temperature, 1710° R.

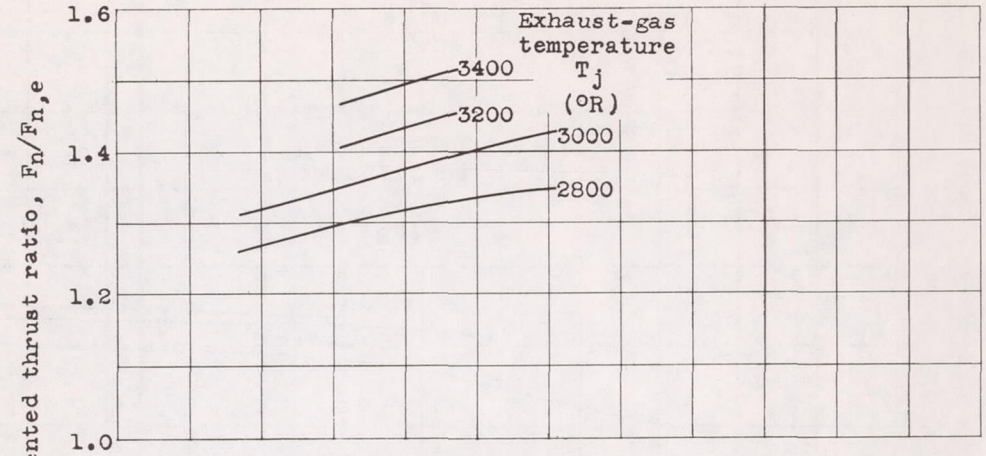

(c) Augmented thrust ratio.

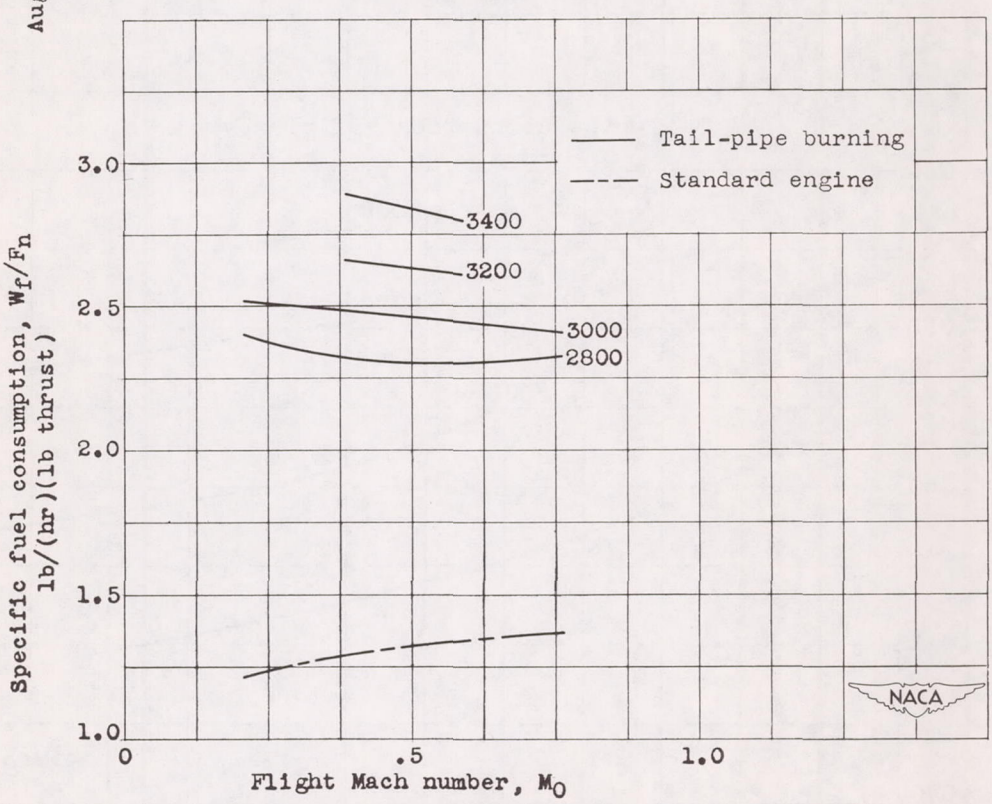

(d) Specific fuel consumption.

Figure 12. - Concluded. Variation of performance with flight Mach number for several exhaust-gas temperatures. Altitude, 25,000 feet; engine speed, 7900 rpm; average turbine-outlet temperature, 1710° R.

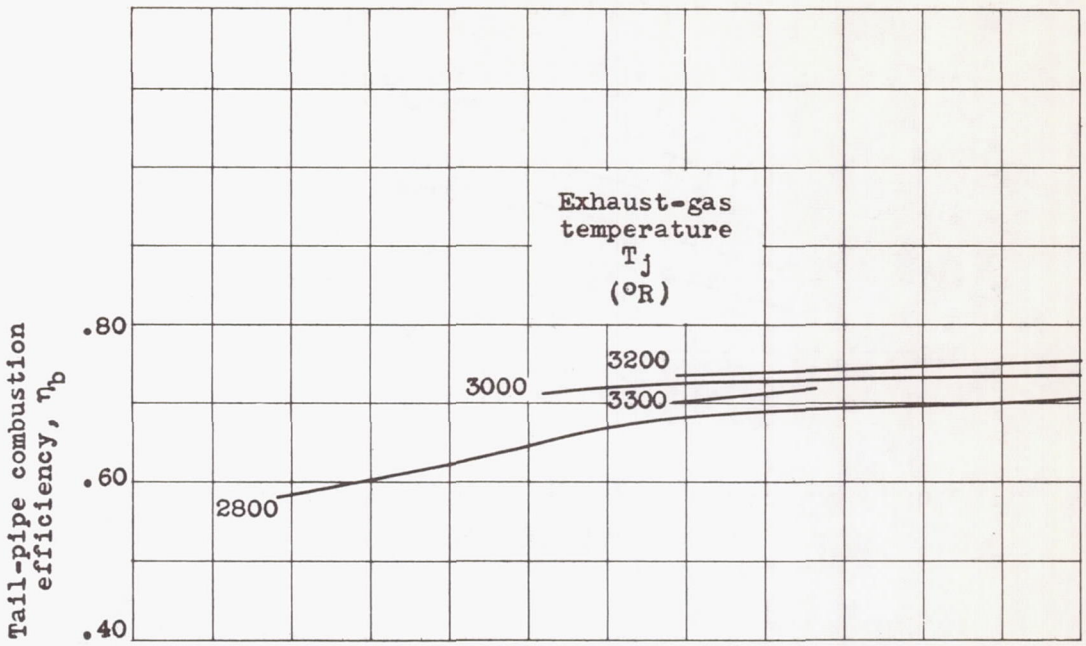

(a) Tail-pipe combustion efficiency.

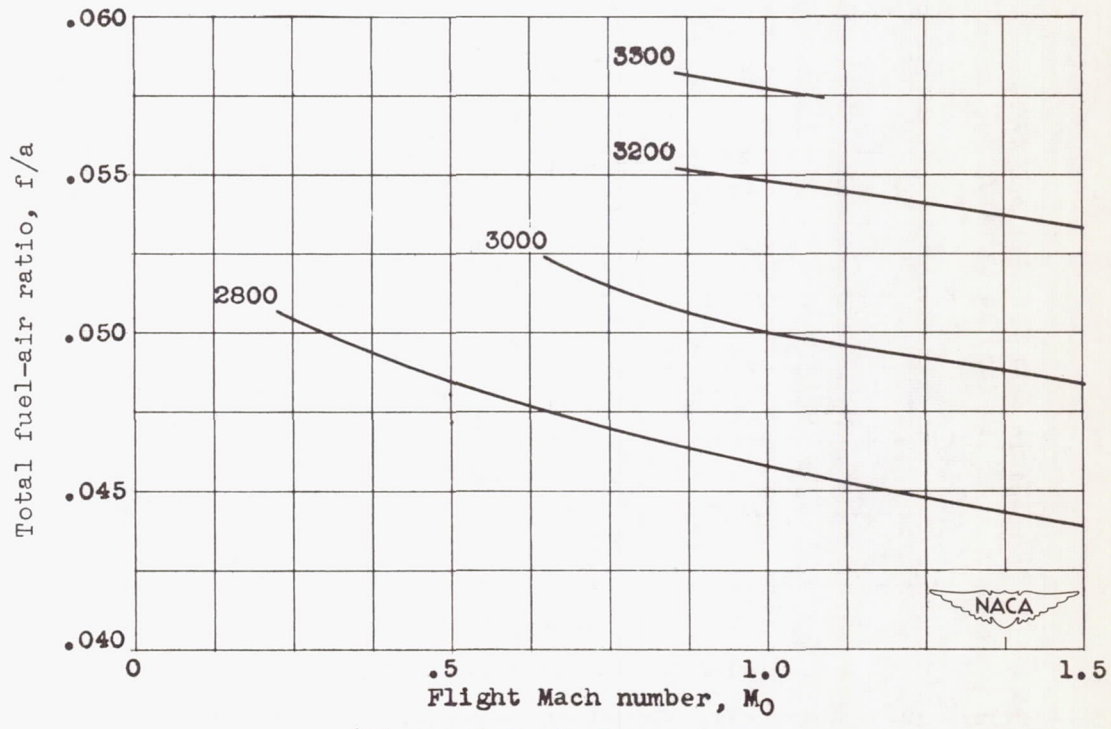

(b) Total fuel-air ratio.

Figure 13. - Variation of performance with flight Mach number for several exhaust-gas temperatures. Altitude, 45,000 feet; engine speed, 7900 rpm; average turbine-outlet temperature, 1710° R.

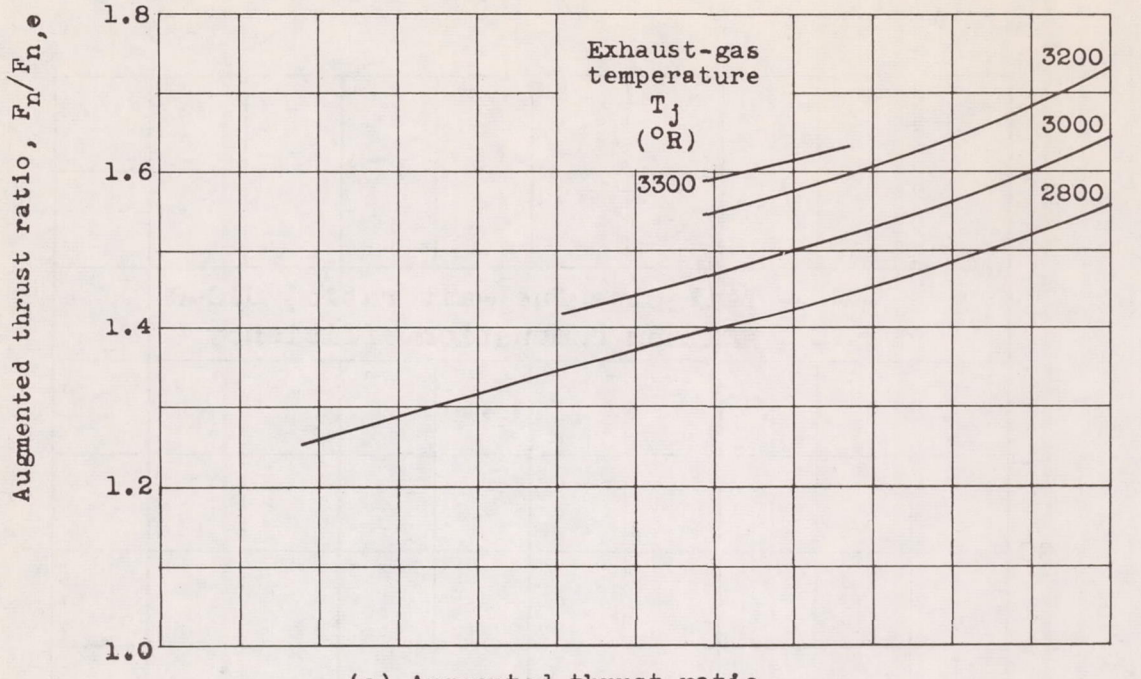

(c) Augmented thrust ratio.

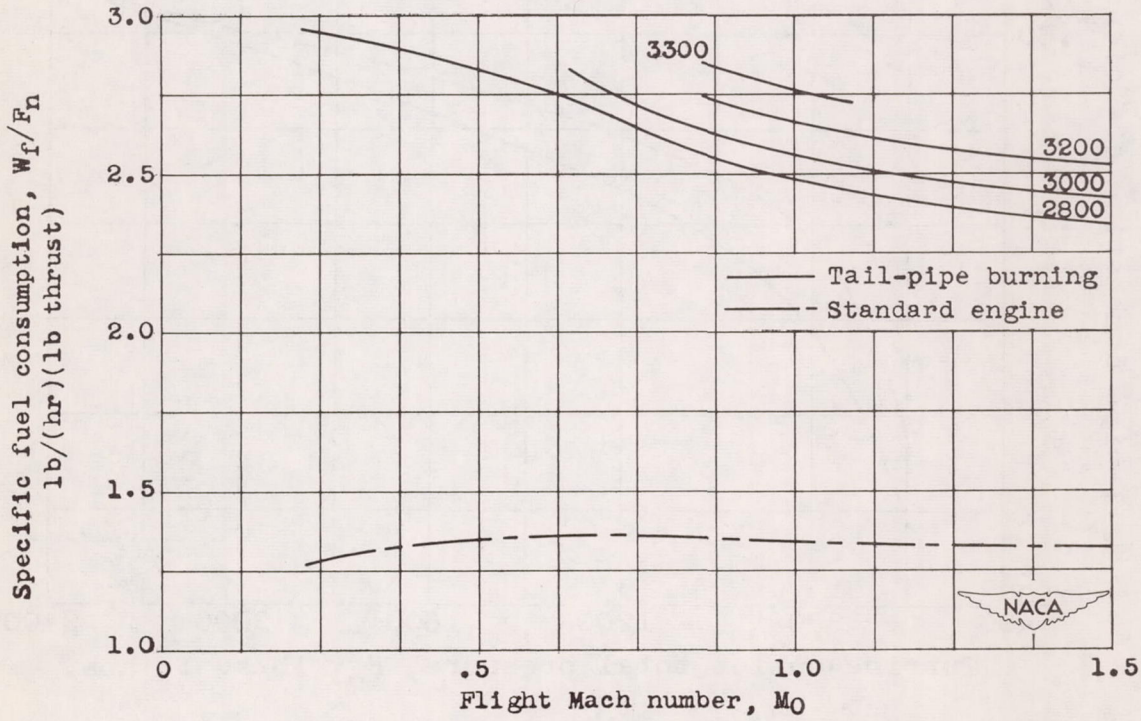

(d) Specific fuel consumption.

Figure 13. - Concluded. Variation of performance with flight Mach number for several exhaust-gas temperatures. Altitude, 45,000 feet; engine speed, 7900 rpm; average turbine-outlet temperature, 1710° R.

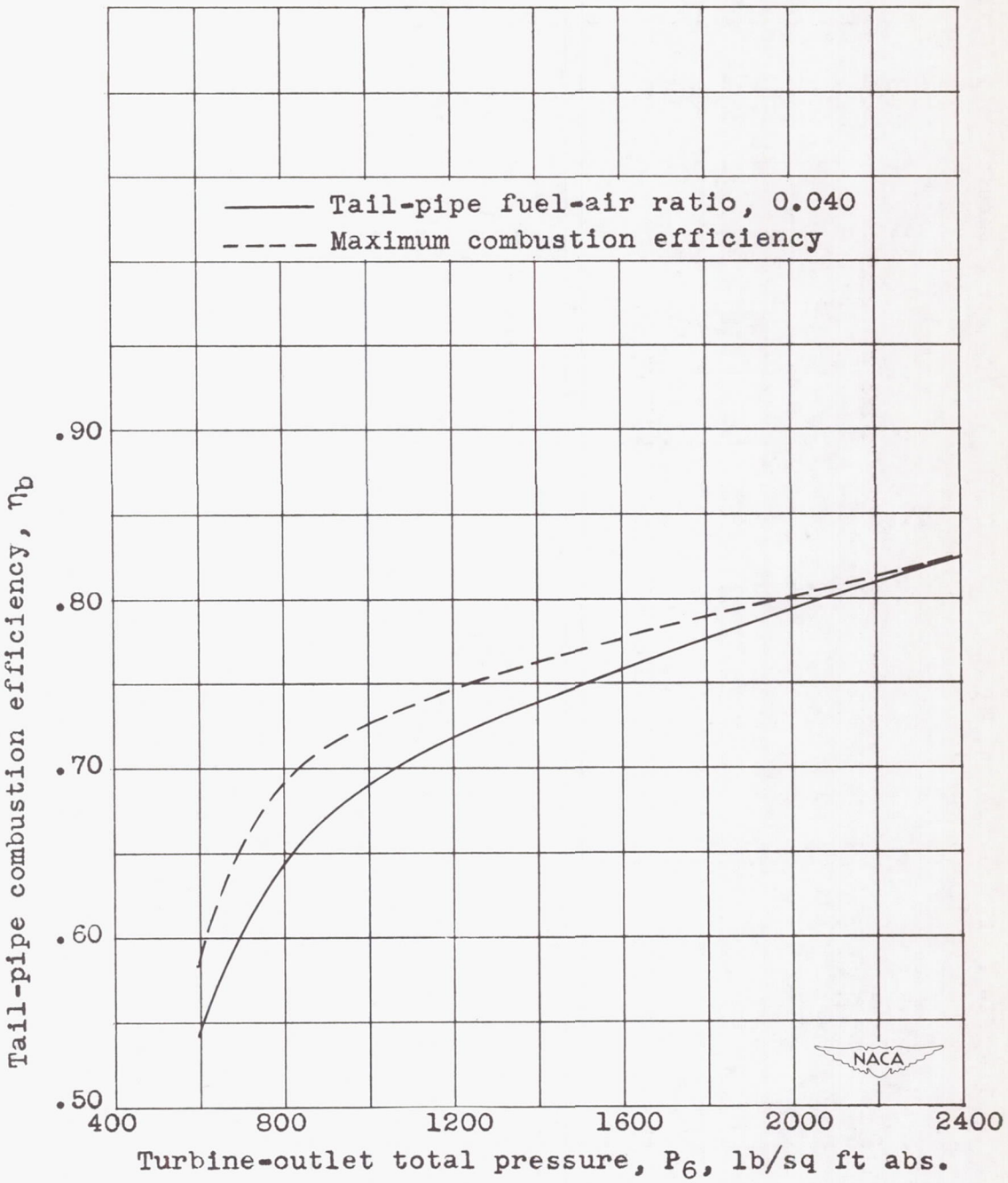

Figure 14. - Effect of turbine-outlet total pressure on tail-pipe combustion efficiency.

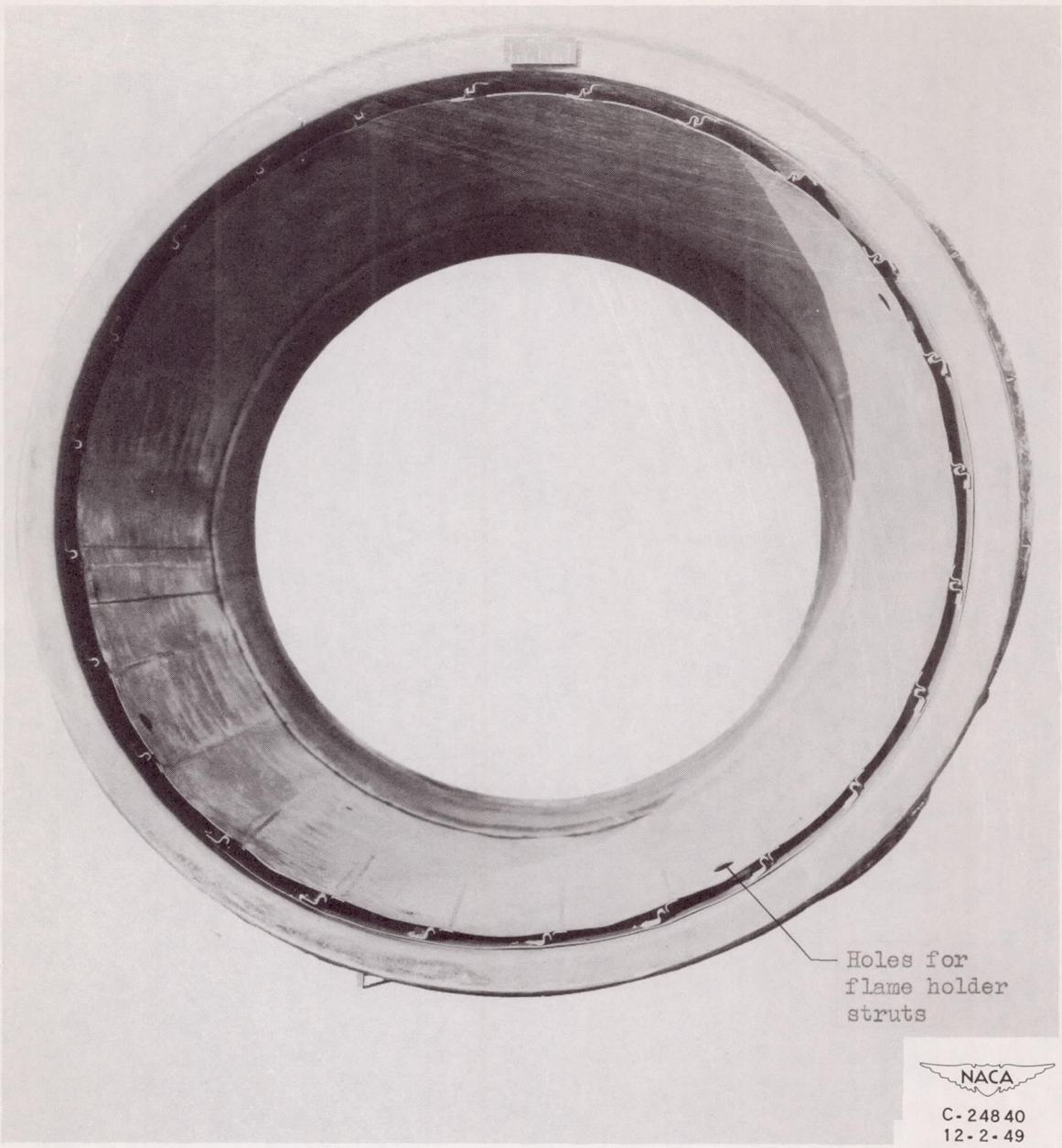

(a) Combustion-chamber-inlet view with flame holder removed showing interlocking support channels used in 32-inch-diameter section.

Figure 15. - Condition of cooling liner after 17 hours of tail-pipe-burner operation.

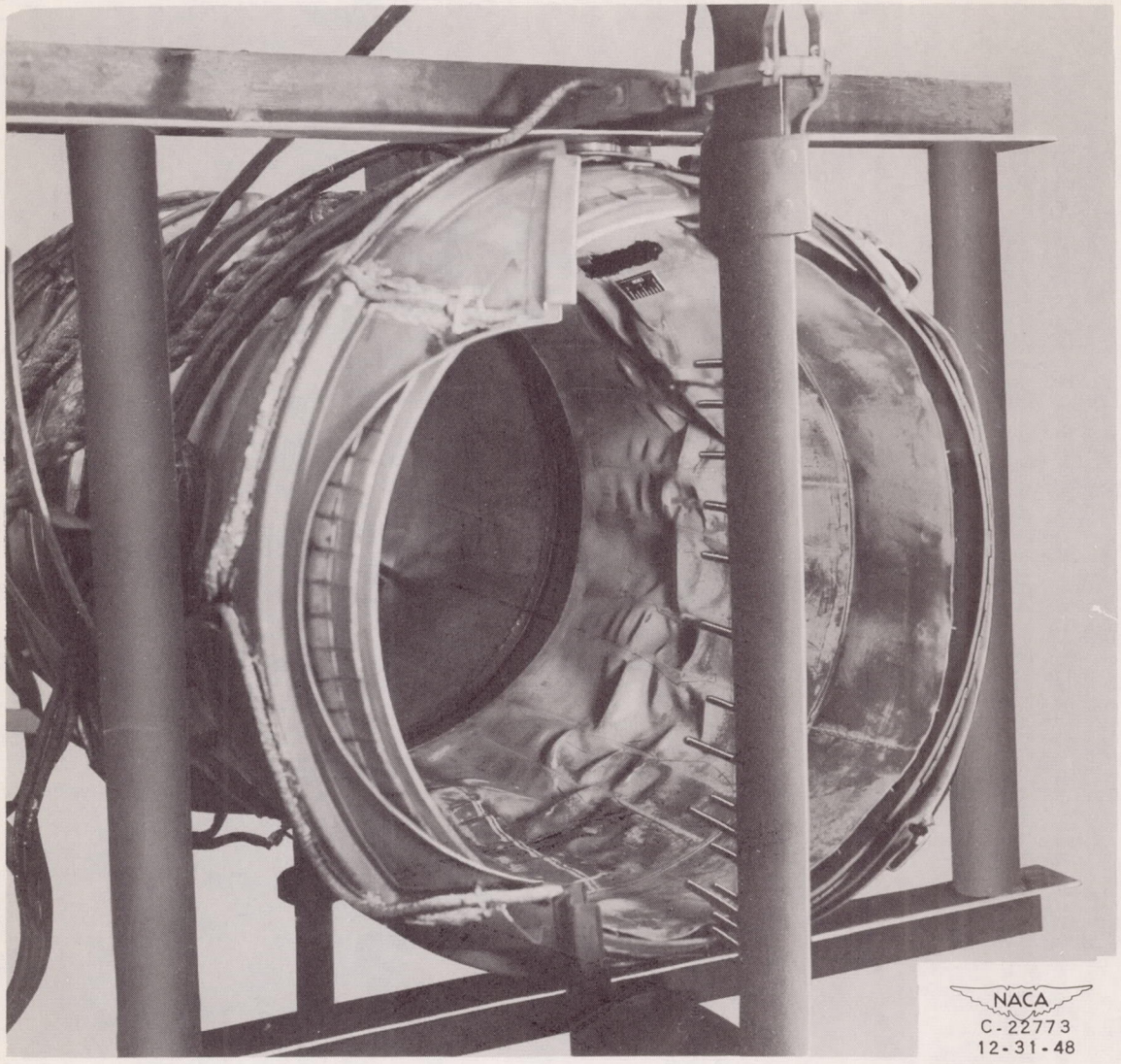

(b) Downstream end of combustion chamber (29-inch-diameter section) viewed through variable-area exhaust nozzle.

Figure 15. - Continued. Condition of cooling liner after 17 hours of tail-pipe-burner operation.

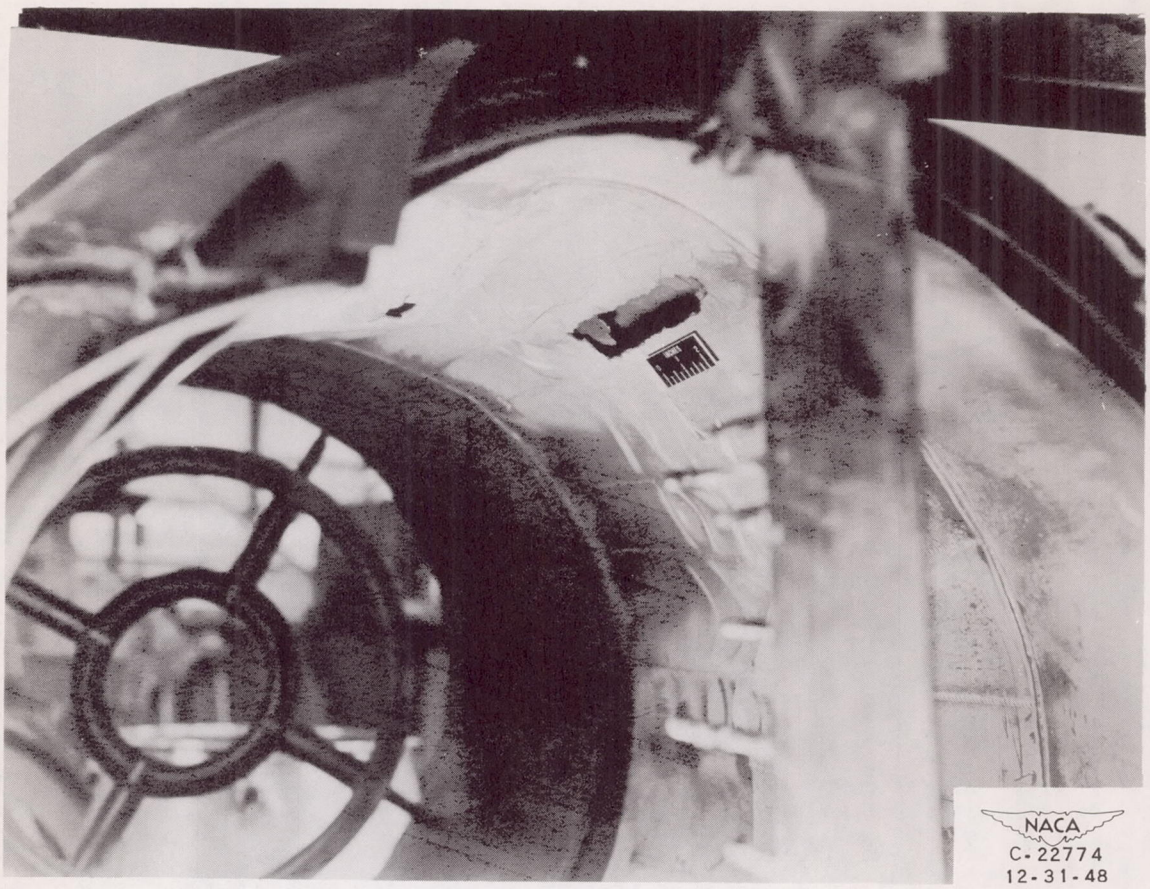

(c) Close-up view of damage to downstream end of liner.

Figure 15. - Concluded. Condition of cooling liner after 17 hours of tail-pipe-burner operation.

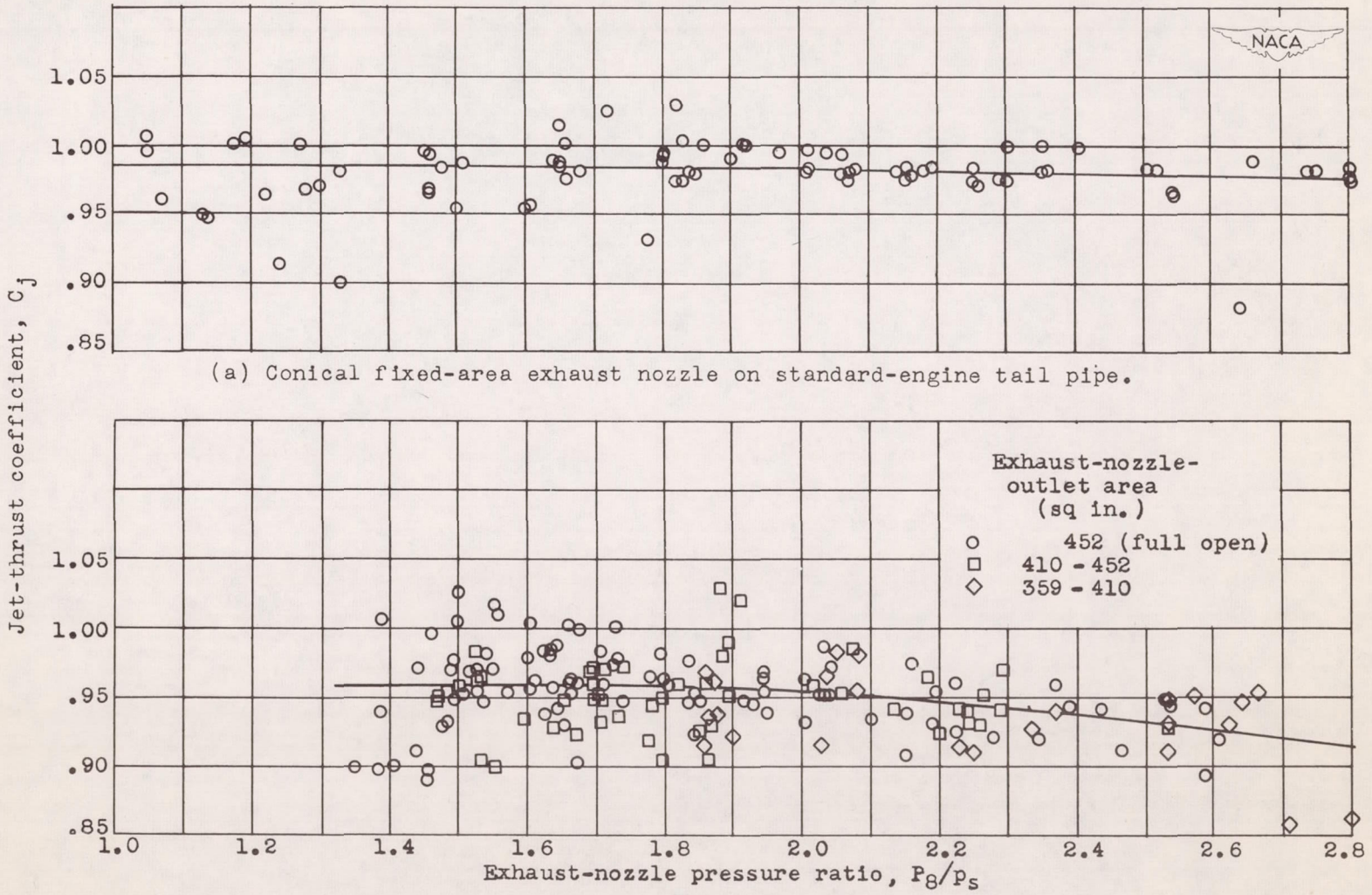

(a) Conical fixed-area exhaust nozzle on standard-engine tail pipe.

(b) Variable-area exhaust nozzle on tail-pipe burner.

Figure 16. - Variation of jet-thrust coefficient with exhaust-nozzle pressure ratio.